OBLIQUE WAVE REFLECTION FROM A MODEL RUBBLE-MOUND BREAKWATER

by

David Arnold Papps

B. E. (hons.), University of Canterbury, 1990

A THESIS SUBMITTED IN PARTIAL FULFILMENT OF

THE REQUIREMENTS FOR THE DEGREE OF

MASTER OF APPLIED SCIENCE

in

THE FACULTY OF GRADUATE STUDIES

Department of Civil Engineering

We accept this thesis as conforming

to the required standard

THE UNIVERSITY OF BRITISH COLUMBIA

January 1992

In presenting this thesis in the partial fulfilment of the requirements for an advanced degree at the University of British Columbia, I agree that the Library shall make it freely available for reference and study. I further agree that permission for extensive copying of this thesis for scholarly purposes may be granted by the head of my department or by his or her representatives. It is understood that copying or publication of this thesis for financial gain shall not be allowed without my written permission.

Department of Civil Engineering

The University of British Columbia

2324 Main Mall

Vancouver, Canada

Date:

January 28, 1992

Abstract

This thesis investigates the characteristics of oblique wave reflection from a model rubble-mound breakwater. An experimental investigation of the reflection of obliquely incident regular, irregular and multi-directional waves, undertaken at the Hydraulics Laboratory of the National Research Council of Canada in Ottawa, is described. A method of analysis, which uses a least squares fit to measurements from three wave probes to estimate the reflection coefficient and the reflected phase lag for regular wave tests, is extended to the case of oblique wave reflection. In the regular wave tests, the wave height, wave period, and angle of incidence were varied in order to determine relationships between the reflection characteristics and parameters describing the incident wave characteristics. Results show that both the reflection coefficient and the reflected phase lag are dependent on the depth to wavelength ratio and the angle of incidence. Reflection coefficients estimated from the analysis of irregular wave tests are also presented and are compared to reflection coefficients measured in regular wave tests, showing good agreement. For multi-directional waves, directional spectra of the incident and reflected wave fields were obtained using a maximum likelihood fit to measurements from five wave probes. Directionality results are presented for one multi-directional wave test showing increased directional spreading of the reflected wave field as compared to the incident wave field.

Table of Contents

List of Tables

List of Figures

page

page

List of Photographs

Acknowledgement

The author would like to thank his supervisor Dr. M. Isaacson for his help and encouragement throughout this project, in particular for his suggestions and guidance in the planning of the experiments, and his advice in the preparation of the thesis.

The author would also like to express his immense gratitude to the Hydraulics Laboratory of the National Research Council of Canada for giving him the opportunity to carry out the experimental work in their excellent facilities. The support of the entire staff at the Hydraulics Laboratory is greatly appreciated. In particular, the author wishes to thank Dr. E. P. D. Mansard, Dr. O. Nwogu and Mr. E. R. Funke for their advice on the experimental work and their efforts in the organisation of the experiments, and Mr. B. Atkins and the technicians at the Hydraulics Laboratory for their assistance in the operation of the experimental programme.

Financial support in the form of a fellowship from the University of British Columbia and a scholarship from the J. Templin Fund is gratefully acknowledged.

Chapter 1
INTRODUCTION

1.1 General

When a train of waves approaches a shoreline or coastal structure a number of physical processes change the form of the waves to produce a particular water surface profile in the vicinity of the water boundary. These processes include wave diffraction around barriers, wave refraction and shoaling over sea bottom topography, wave breaking, and wave run-up on and reflection by boundaries. The combination of these effects, each changing the waves in a particular manner and each to a varying extent, defines the resulting wave condition. Wave reflection contributes greatly to the final wave condition in situations where a body of water is bounded by an artificial breakwater rather than a gently sloping beach. In coastal waters, waves reflected by a shoreline structure or steeply sloping beach can result in agitated sea states which makes the navigation of vessels difficult and which may increase sediment erosion. Within harbours, wave reflection by breakwaters and harbour boundaries can give rise to confused and agitated sea states which may make navigation through entrance channels difficult, and which have an undesirable effect on the motions of moored vessels.

In the design of coastal engineering works it is often desirable to be able to predict the wave condition resulting from a particular breakwater configuration without resorting to a laboratory model. One method of analysing wave conditions in the coastal region, favoured for its efficiency of time and money, is that of numerical modelling. A numerical model can have varying degrees of accuracy, depending on the number and combination of the above processes that are included, and in order to predict wave conditions in a harbour accurately, wave reflection effects should generally be taken into account.

When a regular wave train strikes a boundary it will give rise to a reflected wave train of certain height, direction and phase. For waves reflected by rough sloping surfaces there may be some scattering of direction in the reflected wave, and the reflected wave energy may be shifted to higher frequencies, caused by wave breaking for example. By assuming that a regular wave train reflects from a boundary at an angle equal to the angle of wave incidence and that directional and frequency spreading does not occur, the height and phase of the reflected wave train are sufficient to describe it completely. A more detailed approach would not make the above assumptions but would require that the directional spectrum of the reflected waves be known. The present study is concerned with the characteristics of reflected waves from a straight boundary. Both the above approaches have been considered, with the characteristics of oblique wave reflection from a model rubble-mound breakwater investigated by means of physical modelling.

1.2 Literature Review

The action of normally incident regular waves on rubble-mound breakwaters has been studied quite extensively. Wave reflection under such conditions is generally described by the reflection coefficient K_r, which is defined as the ratio of reflected wave height H_r to incident wave height H_i:

$$K_r = \frac{H_r}{H_i} \tag{1.1}$$

A number of researchers have carried out physical model tests and developed numerical models to determine the reflection coefficient under different conditions.

The use of the surf similarity parameter to determine the reflection characteristics of waves was first suggested by Battjes (1974). This was initially introduced in the context of waves incident on a rigid, plane, impermeable slope extending to deep water and is defined as:

$$\xi = \frac{1.0}{\cot \alpha \sqrt{\frac{H_i}{L_o}}} \tag{1.2}$$

where α is the angle of the slope above horizontal and L_o is the deep water wavelength.

Seelig and Ahrens (1981) have argued that this parameter may be re-defined so as to apply to a rubble-mound breakwater, such that α is taken instead as the angle of the breakwater face above the horizontal. On the basis of laboratory tests, Seelig and Ahrens presented a curve of K_r as a function of the surf similarity parameter. Seelig and Ahrens argue that the calculated value of K_r should be adjusted to account for the relative water depth in front of the breakwater, the thickness of the armour layer and underlayer and the relative size of the armour units.

A review of wave reflections from coastal structures by Allsop and Hettiarachchi (1988) presents plots of K_r as a function of ξ for rubble-mound breakwaters armoured with different types of rock or concrete units.

For the case of reflection of normally incident irregular waves, methods have been proposed (Thornton and Calhoun, 1972, Goda and Suzuki, 1976 and Mansard and Funke, 1980) to measure the spectral density of incident and reflected wave trains in model tests. These spectra can in turn be used to estimate the reflection coefficient as a function of wave frequency, $K_r(f)$:

$$K_r(f) = \sqrt{\frac{S_r(f)}{S_i(f)}} \tag{1.3}$$

where $S_r(f)$ and $S_i(f)$ are the reflected and incident spectral density respectively. An average reflection coefficient $\overline{K_r}$ can also be calculated from the spectra:

$$\overline{K_r} = \sqrt{\frac{(m_o)_r}{(m_o)_i}} \tag{1.4}$$

where $(m_o)_r$ and $(m_o)_i$ are the zeroth moments of the reflected and incident wave spectra respectively.

Kobayashi et al. (1990) used an extension of the methods given by the above authors to separate incident and reflected wave trains in model tests of irregular wave reflection on rough impermeable

slopes. The measured incident and reflected spectral densities were compared to those obtained using a numerical model, showing good agreement for the three tests carried out. Kobayashi used the relationship given in Equation (1.3) to plot reflection coefficient as a function of frequency for his experiments. Measured values of K_r compared well with values provided by the numerical model. Kobayashi also measured and numerically predicted the phase difference between the incident and reflected wave trains at the toe of the slope.

Different studies have concentrated on related effects such as wave transmission through a breakwater and wave run-up on a structure. For example, Sollitt and Cross (1972) presented a study of wave reflection from and transmission through permeable breakwaters. They linearized the unsteady equations of motion for flow through a porous medium to set up a potential flow problem. Their solution to this provides values of K_r and transmission coefficient, K_t. The predicted values of K_r showed reasonable agreement with experimental results for waves of low steepness.

As stated previously, it is necessary to provide details of the reflection of oblique waves in order to describe more fully the process of wave reflection from a structure. Tautenhain et al. (1982) performed experiments to investigate the influence of incidence angle on wave run-up for wave incidence angles between 0° and 35°. It was found that for waves of small angles of incidence the amount of run-up was slightly higher than that for normally incident waves. No results were available on the reflection coefficients occuring in these tests.

Scale effects in rubble-mound breakwater models have been studied by Delmonte (1972) and Wilson and Cross (1972). Delmonte presents experimental results showing the effect of Reynolds number on the transmission coefficient for permeable breakwaters. Reynolds number effects are shown to diminish with increasing wave steepness. Wilson and Cross examine scale effects on reflection and transmission. Scale effects in rubble-mound breakwater models are generally understood to be more important when considering wave transmission rather than wave reflection.

Reynolds number effects in wave reflection tests on rubble-mound breakwaters can be minimised by using a minimum size of breakwater armour corresponding to a critical value of Reynolds number.

1.3 Scope of Present Investigation

A review of the literature has revealed a lack of experimental data on the reflection of obliquely incident waves by coastal structures. This apparent void in the understanding of wave interaction with coastal structures is a major hindrance in the analysis of wave conditions in harbours and marinas. In view of this deficiency the objective of the present investigation is to study the reflection characteristics of waves obliquely incident on a model rubble-mound breakwater.

In particular, the primary objective of this research is to measure the reflection coefficient K_r and phase lag β of the reflected waves due to regular uni-directional incident waves, and to determine relationships providing K_r and β as functions of the incident wave characteristics and the angle of wave incidence.

The secondary objective of this research is to use measurements of the frequency and directional spectra of the reflected wave field to provide comparisons between the characteristics of regular and irregular wave reflection, and to determine the amount of frequency and directional scatter present in the reflected wave field.

Only one particular breakwater type was able to be tested within the scope of the present project. Since rubble-mound breakwaters are the most commonly used form of breakwater used in harbour construction and coastal engineering works, the experiments were carried out with a breakwater of this type. Rubble-mound breakwaters are comprised of one or more layers of large armouring rock over a core of finer stone material, and the particular breakwater characteristics employed in this study were selected in order to model the reflection characteristics of breakwaters commonly

used in practice. It is hoped that the knowledge gained here will be of use in the design and analysis of all breakwater structures.

Chapter 2

METHODOLOGY

2.1 Theoretical Background

In this section, the background theory describing the reflection of oblique regular, irregular and multi-directional waves is presented.

2.1.1 Regular Uni-directional Waves

Figure 2.1 provides a definition sketch for the case of regular uni-directional wave reflection. Using the notation defined in this figure, the water surface elevation η adjacent to a breakwater subjected to obliquely incident regular waves may be expressed as:

$$\eta = \frac{H_i}{2} \cos (kx\cos\theta_i + ky\sin\theta_i - \omega t) + \frac{H_r}{2} \cos (-kx\cos\theta_j + ky\sin\theta_j - \omega t + \beta) \qquad (2.1)$$

where k is the wave number, ω is the wave frequency, and θ_i and θ_j represent the incident and reflected wave angles.

This equation assumes that linear wave theory holds and that there is no directional spreading or frequency scattering of the reflected wave train. If it is further assumed that the angle of incidence is equal to the angle of reflection, then the reflection characteristics of the breakwater may be described by two parameters; the reflection coefficient K_r, and phase lag β. The assumption that linear theory holds is an assumption that is often made in the analysis of water waves and will not be tested in this study, however the validity of the remaining assumptions made in this section will be examined later in this thesis. On the basis of a dimensionless analysis the two quantities K_r and β can be written as functions of independent dimensionless variables, as follows:

$$K_r, \beta = f (\frac{d}{gT^2}, \frac{H_i}{L}, \theta_i, \cot \alpha, \text{type}) \qquad (2.2)$$

where d, g, T and L represent the water depth, the acceleration due to gravity, the wave period, and the wavelength respectively, and the reflection coefficient K_r is defined as: $K_r = H_r / H_i$.

The dimensionless groups are representative of the depth to wavelength ratio, the wave steepness, the angle of incidence, the breakwater slope and the breakwater type (taken to describe rock size and placement, breakwater permeability etc.) respectively.

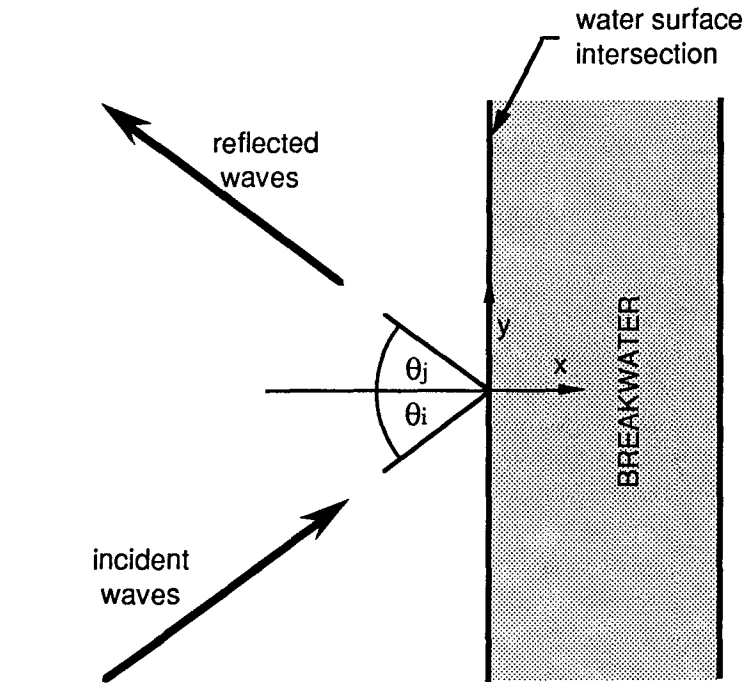

(a) Plan

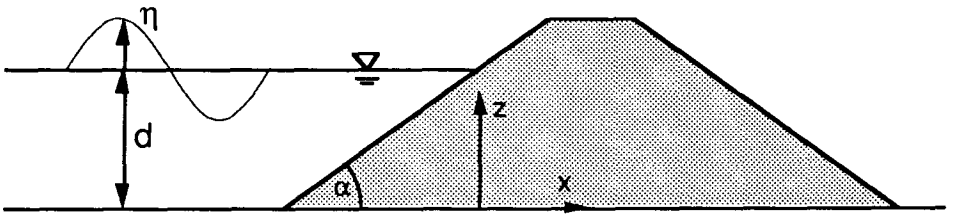

(b) Elevation

Figure 2.1 - Definition sketch of uni-directional wave reflection

2.1.2 Irregular Uni-directional Waves

An irregular signal, such as the water surface elevation signal due to an irregular wave train, may be considered as periodic over a sufficiently long duration and hence may be represented by a Fourier Series which contains components at multiples of the fundamental frequency, f_o. This may be written as follows:

$$\eta(t) = \sum_{n=1}^{\infty} A_n \cos(2\pi n f_o t - \phi_n) \tag{2.3}$$

where A_n are Fourier coefficients representing the amplitudes of each individual frequency component, ϕ_n are the random phase angles of each component, and f_o is the fundamental frequency given by $f_o = 1/T_r$, where T_r is the record length. The variance of the signal may be written as:

$$\sigma_\eta^2 = \sum_{n=1}^{\infty} \frac{1}{2} |A_n|^2 \tag{2.4}$$

Thus $\frac{1}{2}|A_n|^2$ represents the contribution to the variance which is associated with the frequency component nf_o. If the signal period is increased such that $f_o \rightarrow 0$, with the signal now considered to contain a continuous range of frequencies rather than discrete harmonics, the above summation may be replaced with an integral and the variance may be written as:

$$\sigma_\eta^2 = \int_0^{\infty} S_\eta(f)\, df \tag{2.5}$$

where $S_\eta(f)$ is known as the spectral density of η. $S_\eta(f)\,df$ represents the contribution to the variance of the signal due to its content within the frequency range f to f + df. This may be expressed as:

$$S_\eta(f)\,df = \sum_{f_n}^{f_n+df} \frac{1}{2} |A_n|^2 \tag{2.6}$$

From Equation (2.6), a relationship between the Fourier amplitudes and the spectral density can be obtained:

$$A_n = \sqrt{2S_\eta(f).f_o} \tag{2.7}$$

For the case of a reflected wave field, Equation (2.3) may be extended to describe the water surface elevation due to the superposition of incident and reflected wave trains:

$$\begin{aligned}\eta(t) &= \sum_{n=1}^{\infty} A_n \cos(2\pi n f_o t - \phi_n) \\ &= \sum_{n=1}^{\infty} A_{i_n} \cos(2\pi n f_o t - \phi_{i_n}) + \sum_{n=1}^{\infty} A_{r_n} \cos(2\pi n f_o t - \phi_{r_n})\end{aligned} \tag{2.8}$$

It is apparent that, by separating the time series into contributions due to incident and reflected wave trains, the water surface elevation may be described by incident and reflected spectral densities, $S_i(f)$ and $S_r(f)$. If the incident spectral density and reflected spectral density are known, the reflection coefficient as a function of frequency $K_r(f)$, can be found using the result given in Equation (2.7):

$$\begin{aligned}K_r(f) &= \frac{A_r(f)}{A_i(f)} \\ &= \sqrt{\frac{S_r(f)}{S_i(f)}}\end{aligned} \tag{2.9}$$

In addition, an average reflection coefficient $\overline{K_r}$ can be calculated as follows:

$$\overline{K_r} = \sqrt{\frac{(m_o)_r}{(m_o)_i}} \tag{2.10}$$

where $(m_o)_r$ and $(m_o)_i$ are the zeroth moments of the reflected and incident wave spectra respectively.

2.1.3 Irregular Multi-directional Waves

The water surface elevation due to an irregular multi-directional wave train may be expressed as the linear summation of waves in a range of individual directions and a range of individual frequencies:

$$\eta(t) = \sum_{i=1}^{\infty} \sum_{j=1}^{\infty} a_{ij} \cos(k_i x \cos\theta_j + k_i y \sin\theta_j - \omega_i t + \phi_{ij}) \tag{2.11}$$

This sea state may be described using a directional spectral density in a similar way to the description of an irregular, uni-directional sea state by the spectral density. The variance of the water surface elevation signal is considered to be made up of contributions from each frequency range f to f+df, and each direction range θ to $\theta+d\theta$:

$$\sigma_\eta^2 = \int_0^{\infty} \int_0^{2\pi} S_\eta(f,\theta)\, d\theta\, df \tag{2.12}$$

The spectral density of the directional spectrum $S_\eta(f,\theta)$, can be expressed as follows:

$$S_\eta(f,\theta) = S_\eta(f) \,.\, D(f,\theta) \tag{2.13}$$

where $D(f,\theta)$ is the directional spreading function which is a function of frequency as well as direction.

The characteristics of the directional spreading function can be described by the mean direction of wave propogation $\bar{\theta}$ and the standard deviation of the directional distribution σ_θ^2. These are defined as follows:

$$\bar{\theta}\,(f) = \int_{-\pi}^{\pi} D(f,\theta)\, \theta\, d\theta \tag{2.14}$$

$$\sigma_\theta^2(f) = \int_{\bar{\theta}-\pi/2}^{\bar{\theta}+\pi/2} D(f,\theta)\,(\theta-\bar{\theta})^2\,d\theta \qquad (2.15)$$

The standard deviation of the directional distribution provides an indication of the degree of directional spreading. As the value of σ_θ^2 increases the directional spreading becomes greater.

2.2 Laboratory Facilities

The experiments were conducted in the Hydraulics Laboratory of the National Research Council (NRC) of Canada in Ottawa, during July and August of 1991.

2.2.1 Wave Basin

The wave basin used is 50 *m* wide, 30 *m* long, and 3 *m* deep with a 30 *m* segmented wave

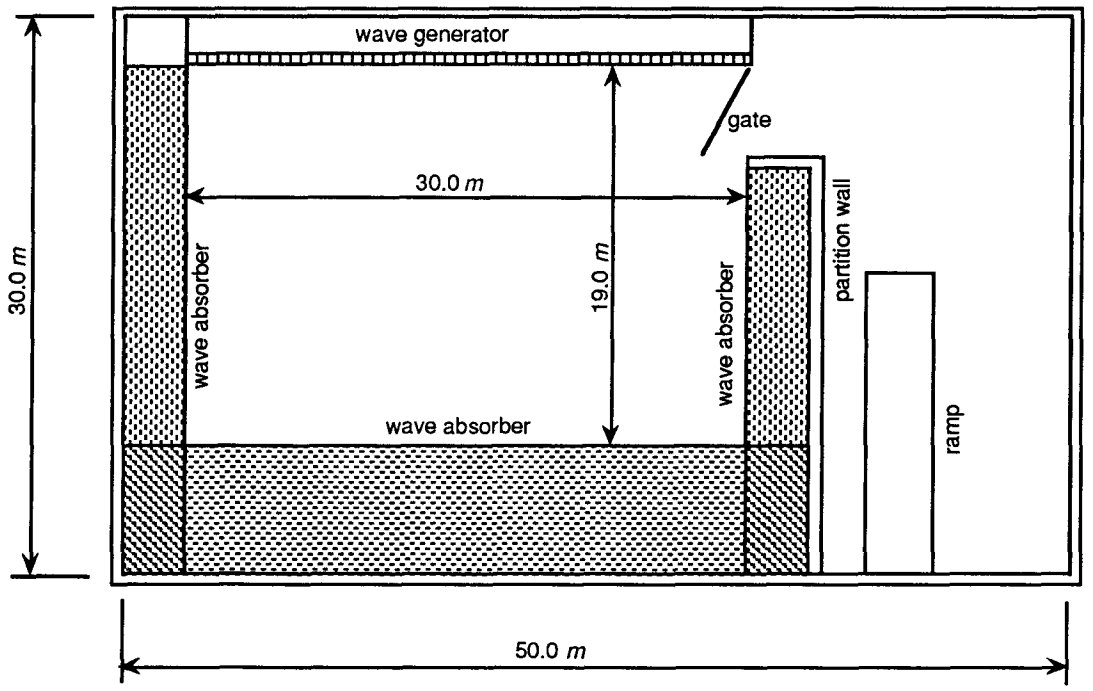

Figure 2.2 - Plan view of the wave basin

generator located along the 50 *m* wall of the basin, as shown in Figure 2.2. The working area of the basin has been reduced to the 30 *m* width of the generator and a length of 19 *m* by the positioning of a partition wall across the basin and the placement of wave absorbers around the periphery of the basin. The absorbers are made up of vertical rows of perforated galvanised steel sheets. The porosity of the sheets decreases closer to the wall in order to extract more and more energy from the wave as it passes through each sheet. This design results in a reflection coefficient of less than 5% for the wave types used in this study (Jamieson and Mansard, 1987).

The normal water depth used in this basin is 2.0 *m*. However, a shallower depth of 0.5 *m* was used in the present study in order to reduce the height of the model breakwater.

2.2.2 Wave Generator

The wave generator is capable of producing regular or irregular, multi-directional or uni-directional waves which can be directed at an angle normal or oblique to the generator face. In this study uni-directional regular, uni-directional irregular, and multi-directional irregular waves were generated over a range of principal directions.

The generator consists of 60 segments, each able to move independently of any other in a specified manner so as to produce the desired wave field. The individual wave boards measure 0.5 *m* in width and 2.5 *m* in height. Each board is driven by a hydraulic actuator with a stroke length of 0.2 *m* and rated static force of 45 *kN*. The actuators are connected to the wave boards by mechanical linkages which provide stroke amplification and can be adjusted to operate the boards in either piston mode, hinged flapper mode, or a combination of both. The 60 actuators are driven by a hydraulic power supply consisting of six pumps, each rated at 50 *US gal/min* and driven with a 75 *kW* motor. The elevation of the wave generator paddles above the basin floor can be varied to suit the particular water depth used. In this study, because of the small water depth, the paddles were lowered to the basin floor.

2.2.3 Wave Generation and Data Acquisition

Wave generation and data acquisition were carried out using the GEDAP software on a microVAX computer. GEDAP is a general purpose software system developed by the NRC Hydraulics Laboratory for the analysis and management of laboratory data, and includes real-time experimental control and data acquisition functions.

The wave generator was controlled with the use of the GEDAP program SWG. The SWG program allows the user to initialize and calibrate the wave generator, to download the driving signals, to adjust the span of the paddle motion, and to start and stop the machine. The 60 individual driving signals must first be synthesized by using one of a number of GEDAP signal generation programs. For uni-directional regular waves program DWREP2B provides the driving signals after requiring the user to select the wave height, wave period, water depth, angle of wave propagation from the generator and also the portions of the generator where the paddles are to be held stationary. For the generation of driving signals for irregular waves and multi-directional waves, alternative GEDAP programs are used, and require the user to specify frequency and directional wave spectra. In order to operate the wave generator the driving signals are downloaded to the generator and the START command is given. The driving signal is smoothly ramped up from zero to full amplitude over a 10 second period by the program SWG in order to protect the wave machine from any sharp transients in the control signal . The generator runs until the STOP command is given.

Data acquisition was carried out on the same VAX computer using the GEDAP program DAS_CMD and a Neff Series 500 data acquisition system. Use of the Neff system allowed 16 signals to be sampled simultaneously through a rack of 16 circuit cards. The signals were each sampled at a rate of 20 samples per second for a duration of 7 minutes, converted from analog signals to digital data, then stored as one GEDAP data file for subsequent analysis. Use of the

program DAS_CMD allows the data acquisition to be synchronised with the start of wave generation.

2.3 Test Set-up

2.3.1 Basin Layout

In order to vary the angle of wave incidence relative to the breakwater, the breakwater was fixed in position and the wave approach direction was varied using the directional wave generator. To attain the required range of incident wave angles of 0 to 60 degrees, the breakwater centreline was aligned at an angle of 45 degrees to the generator face. The basin layout is shown in Figures 2.3 and 2.4 for angles of incidence of 0 and 60 degrees respectively. Photograph 2.1 shows a view of the basin set up for tests with 0 degrees angle of incidence.

These configurations were obtained by considering incident waves with the various directions of approach, and examining regions of reduced incident wave height due to diffraction, and regions where waves reflected off the breakwater are then re-reflected off the generator face. Guidewalls were placed parallel to the direction of wave approach extending from each end of the breakwater to the generator face so as to prevent the incident wave height from being affected by diffraction. Additional wave absorbers were placed in front of the longer guidewall to prevent waves reflected from the breakwater from re-reflecting from this guidewall into the test region. The guidewalls were re-aligned with the direction of incident wave approach for each angle of incidence for the uni-directional wave tests. During the multi-directional wave tests the guidewalls were removed from the basin.

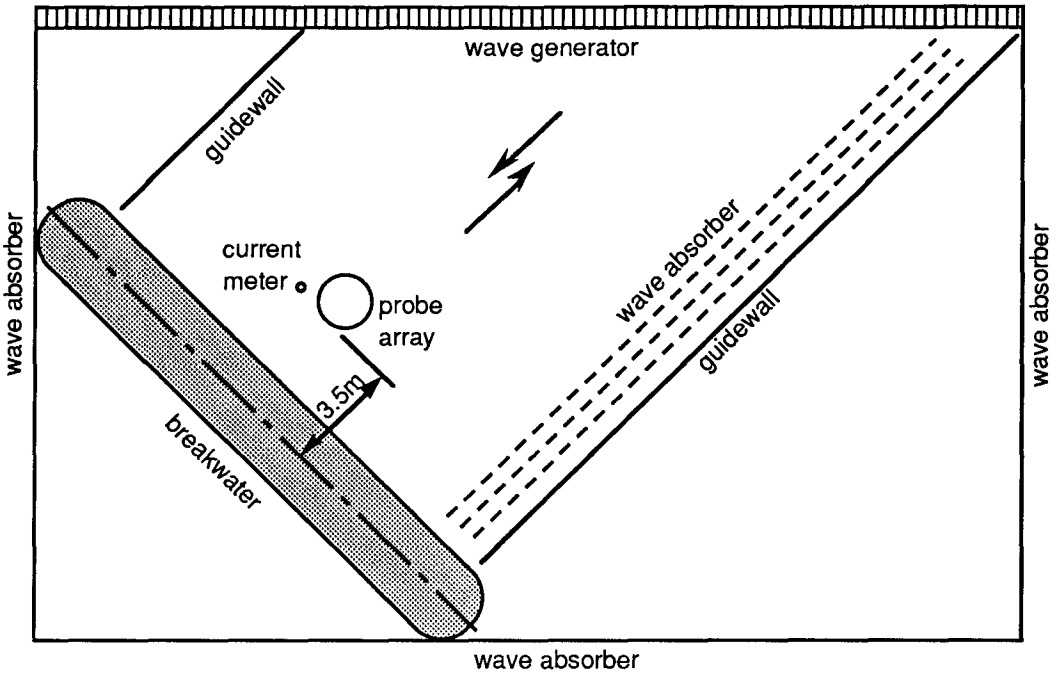

Figure 2.3 - Basin layout for $\theta = 0°$

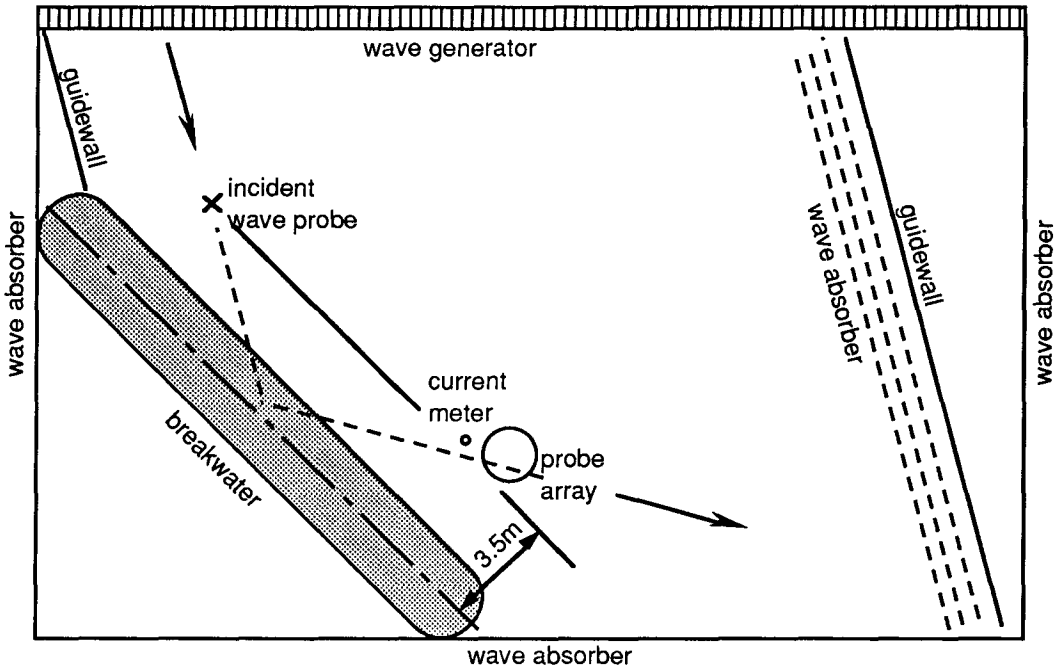

Figure 2.4 - Basin layout for $\theta = 60°$

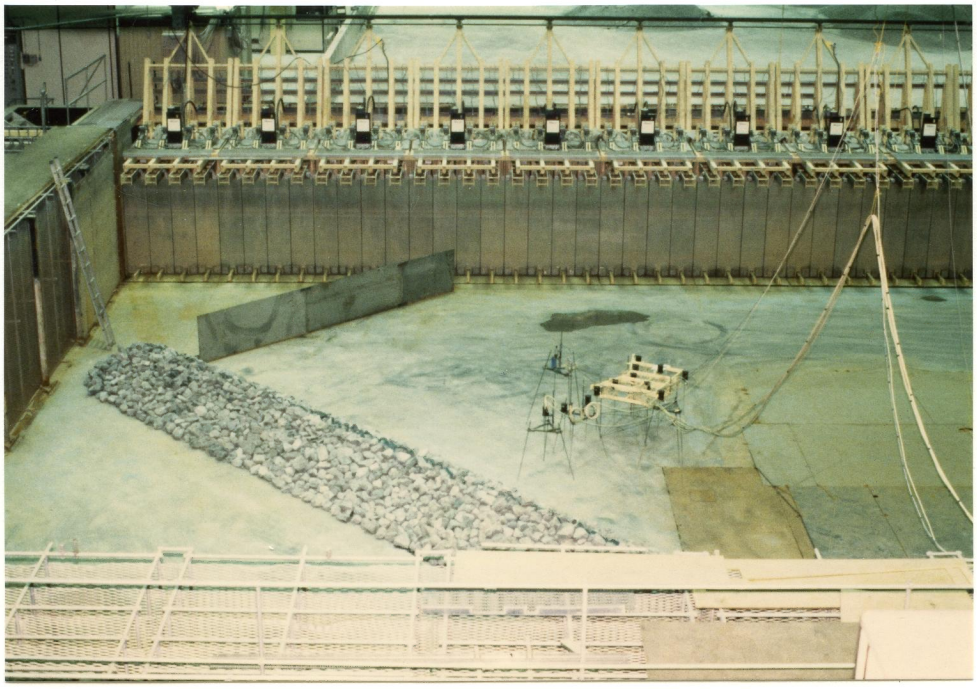

Photograph 2.1 - View of wave basin showing breakwater and guidewall set up for $\theta = 0^\circ$

2.3.2 Breakwater

The model rubble-mound breakwater was designed using methods set out in the Shore Protection Manual (U.S. Army Corps of Engineers 1984) to withstand 0.30 *m* waves without any movement of the armour units or any over-topping, although the largest wave height used in the test programme was less than 0.25 *m*. A secondary design constraint was that the armour units on the breakwater were to be sufficiently large for Reynolds number scale effects to be reasonably small. Personal communications with staff at the National Research Council indicated that a suitable minimum stone weight for this was approximately 200 *g*.

A sketch of the cross-section of the breakwater is shown in Figure 2.5. As indicated in the figure, the breakwater consists of a core, a filter layer and an outer armour layer. The core of finer material was used to reduce energy loss due to wave transmission. The core material was covered by a filter layer consisting of angular rock weighing a minimum of 100 *g*. The outer layer was two stone sizes thick and consisted of angular rock weighing a minimum of 1 *kg*.

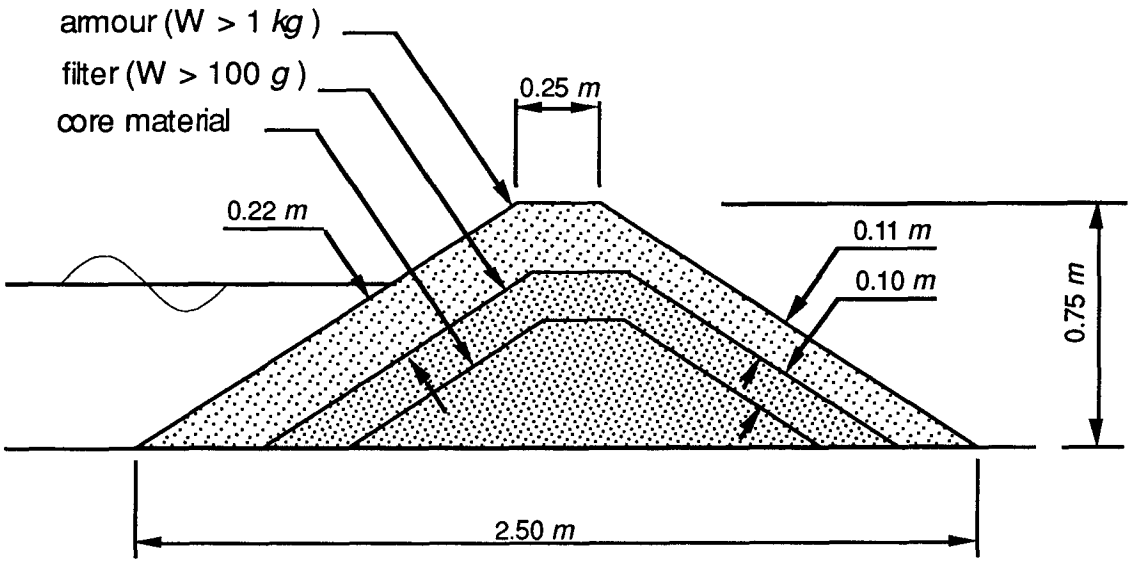

Figure 2.5 - Breakwater cross-section

The breakwater characteristics were as follows:

Breakwater height :	0.75 *m*
Water depth :	0.50 *m*
Crest width :	0.25 *m*
Length :	18 *m*
Front and back slopes :	1:1.5

2.3.3 Wave Measurement

The water surface elevation was recorded at a number of locations in front of the breakwater using twin wire capacitance wave probes. An array of nine probes was used in order to provide data for the directional analysis. The dimensions of the nine probe array are shown in Figure 2.6. Work carried out by Goda and Suzuki (1976) indicates that measurements should be made at a distance of not less than one approximate wave length from the breakwater so as to provide accurate estimates of reflection coefficients. For this reason the wave probe array was placed such that the distance from the intersection of the water surface with the breakwater face to the nearest wave

probe in the array was 3 *m*, which corresponds to one average wavelength. The approximate positions of the wave probe array for angles of incidence 0° and 60° are shown in Figures 2.3 and 2.4. A view of a test in progress, showing the position of the wave probe array, is given in Photograph 2.2. In this photograph the incident wave parameters are: $\theta = 45°$, T = 1.6 *s*, H = 0.15 *m*.

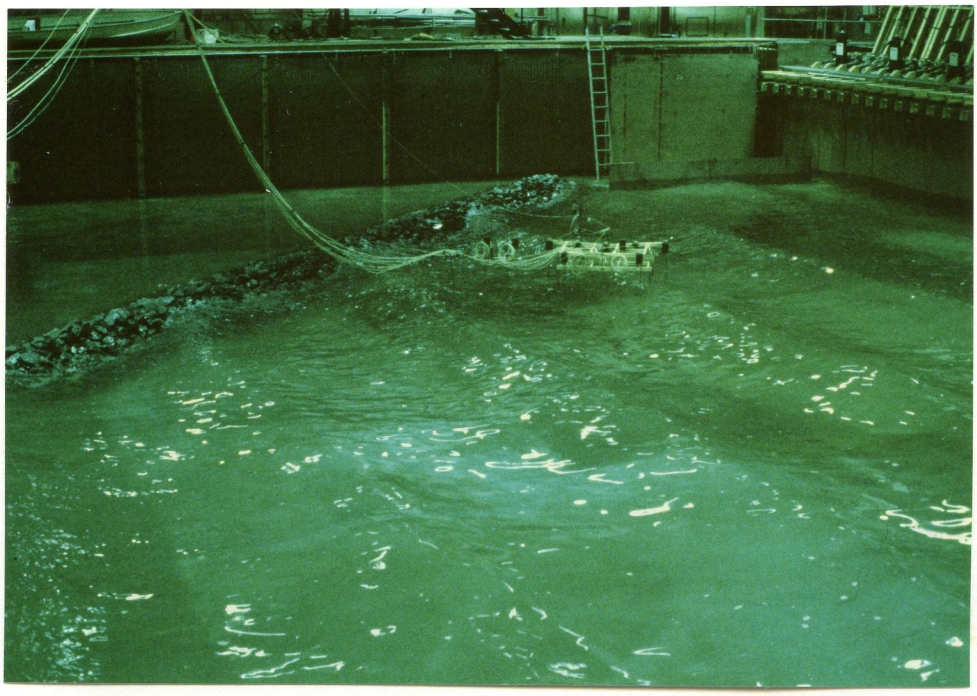

Photograph 2.2 - View of test 17 with $\theta = 45°$

The reflection analysis used for uni-directional, regular waves required water surface elevation signals measured at three locations aligned perpendicular to the breakwater face. Consequently, the array was aligned such that the three wave probes nearest the breakwater, which in Figure 2.6 are labelled "1", "2", and "3", lay precisely on a line perpendicular to the breakwater face. These three probes were used for the uni-directional, regular wave analysis and for the uni-directional, irregular analysis.

Apart from measurements using the wave probe array, measurements were also made using a single wave probe placed in front of the breakwater, as indicated by Figure 2.4, so as to measure the incident wave height on the wave orthogonal that was reflected through the probe array.

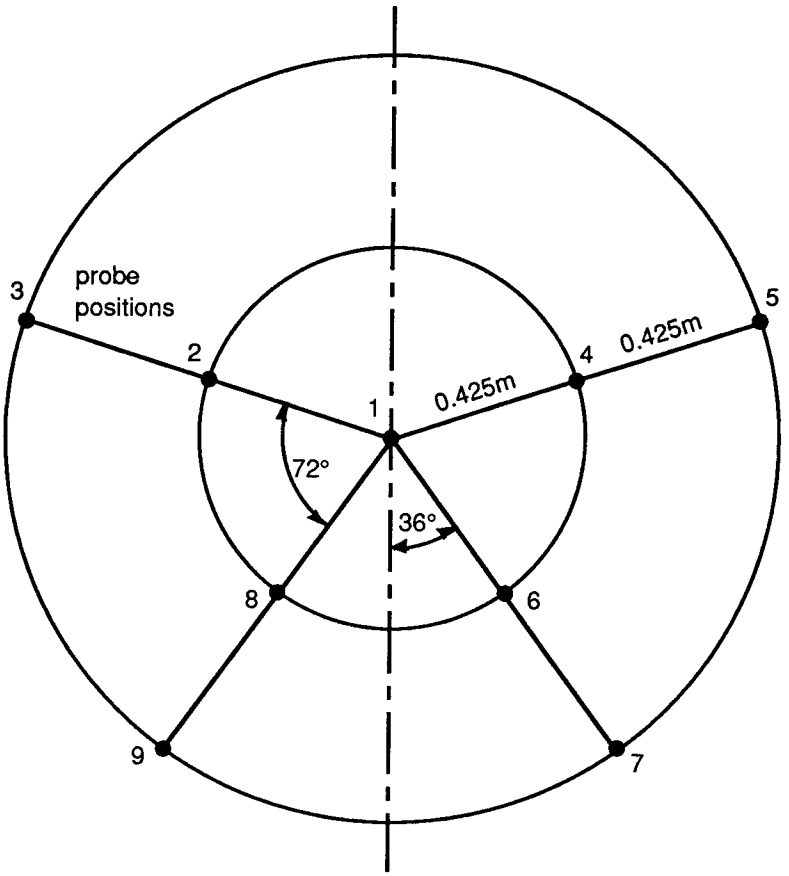

Figure 2.6 - Approximate dimensions of the wave probe array

Measurements for the directionality analysis were made using the nine-probe array shown in Figure 2.6. The dimensions of this array were chosen to match the array used by Nwogu (1989) so that the directional analysis methods used by Nwogu in his multi-directional wave tests could be used in this study. The location of the array is shown in Figures 2.3 and 2.4. In addition to the wave probe array, an alternative set of directional wave measurements were made using a Delft bi-axial current meter, with water surface elevation measurement, located adjacent to the wave probe array, (see Figures 2.3 and 2.4). This was mounted on a separate tripod stand which was located

some distance from the wave probe array and any other metallic objects to minimise the possibility of signal noise due to electromagnetic interference.

All the wave probes were calibrated at the start of each day of testing by raising and lowering the probes by a known distance and recording the signal voltage at these two positions as well as the operating position. A linear relationship between signal voltage and water surface elevation was observed, with very small error, which was typically less than 0.5 mm, and there was good repeatibility of calibration coefficients from calibration to calibration.

2.4 Test Programme

The waves used in the test programme are outlined in Table 2.1 below:

test number	wave period (s)	wave height (m)	angle of incidence (deg.)	d/gT^2 (or d/gT_p^2)	H/L (or H_s/L_p)	wave type
1	1.0	0.10	0, 30, 45, 60	0.051	0.066	regular
2	1.2	0.10	0, 30, 45, 60	0.035	0.049	regular
3	1.6	0.10	0, 30, 45, 60	0.020	0.032	regular
4	2.0	0.10	0, 30, 45, 60	0.013	0.025	regular
5	2.4	0.10	0, 30, 45, 60	0.009	0.020	regular
6	1.6	0.05	0, 45	0.020	0.016	regular
7	1.6	0.15	0, 45	0.020	0.049	regular
8	1.6	0.18	0, 45	0.020	0.058	regular
9	1.6	0.19	0, 45	0.020	0.062	regular
10	$T_p = 1.6$	$H_s = 0.06$	0, 45	0.020	0.019	irregular
11	$T_p = 1.6$	$H_s = 0.12$	0, 45	0.020	0.039	irregular
12	$T_p = 1.6$	$H_s = 0.15$	15, 30	0.020	0.048	uni-directional, irregular
13	$T_p = 1.6$	$H_s = 0.15$	15, 30	0.020	0.048	multi-directional, irregular

Table 2.1 - Test Programme

It was expected that the wave parameters that would have the greatest influence on the reflection characteristics would be the wavelength L, the wave height H, and the angle of incidence θ. For this reason, the water depth was held at a constant value of $d = 0.5$ *m* for all waves generated, and the wave period, the wave height and the angle of incidence were varied.

Analysis of regular wave reflection was intended to reveal relationships between the parameters K_r and β and the two dimensionless wave parameters representing wave steepness and depth to wavelength ratio. With this in mind, the following set of tests were undertaken, corresponding to tests 1 to 9 in Table 2.1:

a) The effects of depth to wavelength ratio were examined in tests 1 to 5 by changing the wave period and keeping other parameters constant. Values of wave period ranging from T = 1.0 *s* to 2.4 *s* were used which provided values of depth to wavelength ratio ranging from $d/gT^2 = 0.009$ to 0.051.

b) The effects of angle of wave incidence were examined by repeating these tests for the four angles of incidence: $\theta = 0°, 30°, 45°, 60°$.

c) The effects of wave steepness were examined in tests 6 to 9 by keeping the wave period constant at T = 1.6 *s* and changing the wave height. Values of wave height ranging from H = 5 *cm* to 19 *cm* were used which provided values of wave steepness ranging from H/L = 0.016 to 0.066. These tests were carried out with two angles of incidence: $\theta = 0°, 45°$

Tests 10 and 11 in Table 2.1 represent the phase of testing with irregular, uni-directional waves. These tests were undertaken in order to examine how adequately the results obtained from the regular wave experiments described the characteristics of irregular wave reflection. The irregular wave trains were approximately described by a Bretschneider spectrum given by:

$$S_\eta(f) = \frac{5\,H_s^2}{16\,f_p}\,\frac{1}{(f/f_p)^5}\,\exp\left\{-\frac{5}{4}\left(\frac{f}{f_p}\right)^{-4}\right\} \qquad (2.16)$$

where H_s is the significant wave height and f_p is the peak frequency of the spectrum ($f_p = 1/T_p$). The characteristics of the irregular waves were chosen so as to allow comparisons to be made between the irregular wave results and results from selected regular wave tests. Tests 10 and 11,

with significant wave heights $H_S = 6\ cm$ and 12 *cm* and peak period $T_p = 1.6\ s$, were generated with two angles of wave incidence: $\theta = 0°$ and 45°.

One of the objectives of this research was to search for and quantify any directional spreading in the waves reflected from the breakwater. As an extension of this a series of multi-directional testing was undertaken. Both uni-directional (test 12) and multi-directional (test 13) wave trains were generated with the same frequency spectrum to compare the spreading of the reflected wave field for uni-directional and multi-directional incident waves. These waves were generated in two principal directions, $\theta_p = 15°, 30°$.

In order to provide data on the incident wave field in the absence of breakwater reflections, the entire test programme for all angles of incidence was performed twice; firstly without the breakwater in place and secondly with the breakwater in place. During the first phase of tests the guidewalls were left in place and reflections were suppressed by wave absorbers around the periphery of the basin. Full measurement of the water surface elevation and water particle velocities, as described in Section 2.3.3, was made for both phases of testing.

Chapter 3

ANALYSIS TECHNIQUES

3.1 Regular Uni-Directional Reflection Analysis

For the case of regular, uni-directional wave reflection, a method of analysis was required that provided three wave reflection parameters: the incident wave height, the reflection coefficient, and the reflection phase lag, from measurement of water surface elevations. In this project a method was used which applies a least squares technique to measurements from three wave probes. The application of this method to normal wave reflection has been described by Isaacson (1991) and Mansard and Funke (1980) and its extension to oblique wave reflection has been indicated by Isaacson (1991).

3.1.1 Derivation of Least Squares Method

The water surface elevation in front of the breakwater is assumed to correspond to the superposition of sinusoidal incident and reflected wave trains. The reflected wave train is assumed to reflect away from the breakwater at an angle of reflection equal to the angle of incidence. To describe the wave field, Equation (2.1) can be re-written as:

$$\eta = a_i \cos (kx \cos\theta + ky \sin\theta - \omega t) + a_r \cos (-kx \cos\theta + ky \sin\theta - \omega t + \beta) \qquad (3.1)$$

where a_i and a_r are the amplitudes of the incident and reflected wave trains respectively and β is the phase difference between the two trains at the position $x = 0$. The origin of the x axis is defined as the intersection of the still water level and the breakwater face. θ is the angle of wave incidence on the breakwater and k and ω are the wave number and angular frequency, related by the dispersion relation:

$$\omega^2 = gk \tanh(kd) \qquad (3.2)$$

where g is the acceleration due to gravity and d is the water depth. Assuming ω is known from measurements of the wave period, there are three unknowns: a_i, a_r, and β.

Equation (3.1) is applied at a series of known probe positions on the x axis; x_n, y_n, n = 1, 2, 3 ... and $y_n = 0$. The location along the x axis may be written in terms of the location of the first probe x_1 and the intervals between the probes:

$$x_n = x_1 + \lambda_n \tag{3.3}$$

where λ_n is the distance in the x coordinate between the n^{th} probe and the first probe, and $\lambda_1 = 0$. It is convenient to write this in dimensionless form as:

$$kx_n \cos\theta = kx_1 \cos\theta + \Delta_n \tag{3.4}$$

where Δ_n is the dimensionless distance between the n^{th} probe and the first.

$$\Delta_n = k\lambda_n \cos\theta \tag{3.5}$$

Applying Equation (3.1) at each of the probe locations gives:

$$\begin{aligned} \eta_n &= a_i \cos (kx_n\cos\theta + ky_n\sin\theta - \omega t) + a_r \cos (-kx_n\cos\theta + ky_n\sin\theta - \omega t + \beta) \\ &= a_i \cos (kx_1\cos\theta + \Delta_n - \omega t) + a_r \cos (-kx_1\cos\theta - \Delta_n - \omega t + \beta) \end{aligned} \tag{3.6}$$

The actual measurements at the probe locations will provide corresponding amplitudes and relative phases, such that the measured elevation at the n^{th} probe may be written as:

$$\begin{aligned} \eta_n^{(m)} &= A_n \cos(\omega t - \phi_n) \\ &= A_n \cos(\omega t - \phi_1 - \delta_n) \end{aligned} \tag{3.7}$$

where A_n is the measured amplitude of the water surface at the n^{th} probe, ϕ_1 is the absolute phase of the first probe which need not be measured, and δ_n is the measured phase of the n^{th} wave record relative to the first, so that $\delta_n = \phi_n - \phi_1$.

It is convenient to describe the water surface elevation in complex notation in order to simplify the algebra, with the real parts of complex expressions corresponding to the physical quantity described. Equation (3.6) expressing the water surface elevation in terms of the unknown incident and reflected wave parameters can be written in complex form as:

$$\eta_n = \left\{ a_i\, e^{i(kx_1\cos\theta+\Delta_n)} + a_r\, e^{i(-kx_1\cos\theta-\Delta_n+\beta)} \right\} e^{-i\omega t} \tag{3.8}$$

The measured water surface elevation can be written in complex form as:

$$\eta_n^{(m)} = A_n\, e^{i(\phi_1+\delta_n)}\, e^{-i\omega t} \tag{3.9}$$

Equations (3.8) and (3.9) can be re-written in terms of complex amplitudes:

$$\eta_n = \left\{ b_i\, e^{i\Delta_n} + b_r\, e^{-i\Delta_n} \right\} e^{-i\omega t} \tag{3.10}$$

$$\eta_n^{(m)} = B_n\, e^{-i\omega t} \tag{3.11}$$

where

$$b_i = a_i\, e^{i(kx_1\cos\theta)} \tag{3.12}$$

$$b_r = a_r\, e^{i(-kx_1\cos\theta+\beta)} \tag{3.13}$$

$$B_n = A_n\, e^{i(\phi_1+\delta_n)} \tag{3.14}$$

The sum of the squares of the error between the complex amplitudes of the assumed and measured elevations may be written from Equations (3.10) and (3.11) as:

$$E^2 = \sum_{n=1}^{3} [b_i\, e^{i\Delta_n} + b_r\, e^{-i\Delta_n} - B_n]^2 \tag{3.15}$$

The error of fit is minimised with respect to the required complex unknowns b_i and b_r by setting $\partial(E^2)/\partial b_i$ and $\partial(E^2)/\partial b_r$ in turn to zero. This gives rise to two complex equations for b_i and b_r:

$$\sum_{n=1}^{3} e^{i\Delta_n} [b_i e^{i\Delta_n} + b_r e^{-i\Delta_n} - B_n] = 0 \tag{3.16}$$

$$\sum_{n=1}^{3} e^{-i\Delta_n} [b_i e^{i\Delta_n} + b_r e^{-i\Delta_n} - B_n] = 0 \tag{3.17}$$

Solving these two equations provides b_i and b_r in terms of B_n and thereby provides a_i, a_r and β in terms of A_n. This solution was expressed by Isaacson (1991) as :

$$a_i = |X_i| \tag{3.18}$$

$$a_r = |X_r| \tag{3.19}$$

$$\chi = \text{Arg}(X_i) - \text{Arg}(X_r) \tag{3.20}$$

$$\beta = 2kx_1 - \chi \pm 2\pi m \tag{3.21}$$

where m is any integer, usually chosen such that $0 \leq \beta < 2\pi$, and where

$$X_i = \frac{s_2 s_3 - 3s_4}{s_5} \tag{3.22}$$

$$X_r = \frac{s_1 s_4 - 3s_3}{s_5} \tag{3.23}$$

$$s_1 = \sum_{n=1}^{3} e^{i2\Delta_n} \tag{3.24}$$

$$s_2 = \sum_{n=1}^{3} e^{-i2\Delta_n} \tag{3.25}$$

$$s_3 = \sum_{n=1}^{3} A_n e^{i(\delta_n + \Delta_n)} \tag{3.26}$$

$$s_4 = \sum_{n=1}^{3} A_n e^{i(\delta_n - \Delta_n)} \tag{3.27}$$

$$s_5 = s_1 s_2 - 9 \tag{3.28}$$

Simple substitution of measured quantities into Equations (3.24) to (3.28) and trivial calculations using Equations (3.18) to (3.23) will yield the incident and reflected wave heights and the reflection phase lag. Hence from measurements of the amplitudes and the phases of three wave probes aligned perpendicular to the breakwater the basic reflection characteristics K_r and β are able to be calculated.

3.1.2 Application of Least Squares Method

The least squares method was applied to signals measured at locations on a perpendicular line to the breakwater at distances from the breakwater of approximately 3.00 *m*, 3.46 *m*, and 3.89 *m*. Extensive numerical testing of this method by Isaacson (1991) shows that the accuracy of the method decreases when the spacings between probes one and two and probes two and three are equal. Therefore, in this project the centre probe was not placed exactly mid-way between the two exterior probes, but was located such that $\lambda_2 = 0.52\ \lambda_3$. For this ratio of probe spacings, Isaacson found that the method should have good accuracy.

The amplitude and phases of the measured signals were obtained using the GEDAP program APHRES. This program performs a nonlinear optimization to fit a sinusoidal curve to the data. In the program, three parameters: the amplitude A, phase angle β, and frequency f, are optimized in an iterative process. Convergence is deemed to have been obtained when the the change in parameters between successive iterations falls below a user specified limit.

This method was used in preference to a Fourier analysis method for two reasons:

1) Fourier analysis methods are sensitive to record length and the number of sample points, whereas the program APHRES can be used on short length records with confidence. The eventual record length used in the analysis of the regular waves was only 10 seconds.

2) Accurate measurement of phase angles is needed for the least squares reflection analysis. An initial comparison of sinusoidal fitting programs with Fourier analysis programs indicated that the former provides more accurate phase angle results.

It was found that APHRES did not converge to give reasonable results when the mean water level fluctuated significantly with time due to low frequency waves. This was not the case when short record lengths were used in the analysis.

Once the three amplitudes A_1, A_2, A_3 and the two phase differences δ_1, δ_2 were known for each wave record, these five quantities, together with the angle of incidence θ, wave period T, water depth d, and probe positions x_1, x_2, x_3 were specified as input to a simple FORTRAN program which used Equations (3.18) to (3.28) to calculate a_i, a_r and β.

Rather than use a_i to calculate the reflection coefficient K_r, the incident weave height measured at

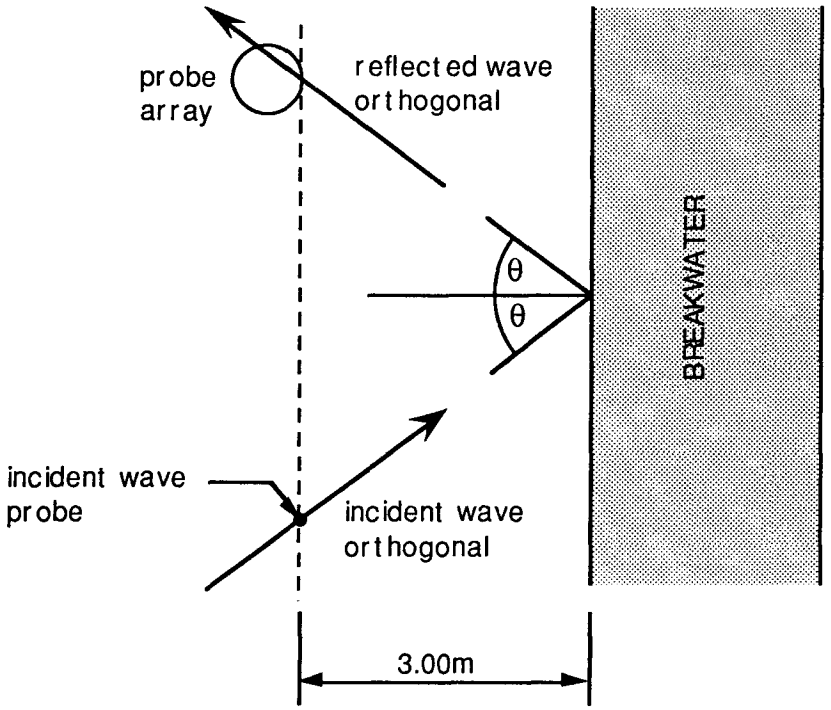

Figure 3.1- Location of wave probes

the incident wave probe in the absence of the breakwater has instead been used. This probe was located on the wave orthogonal that was reflected through the probe array, as is shown by Figure 3.1. It is expected that there is generally a spatial variation in the incident wave height, and that the use of the height measured at the incident wave probe is more appropriate.

3.2 Irregular Wave Analysis

Analysis of the irregular wave tests required that the spectral density of the incident and reflected wave trains be obtained. The spectral density, described by Equations (2.5) and (2.6) in Section 2.1.2, was calculated using the GEDAP program VSD. The reflection coefficient as a function of frequency was then calculated by dividing the reflected spectral density function by the incident spectral density function, as is described by Equation (2.9). Equation (2.10) was used to calculate the average reflection coefficient $\overline{K_r}$, from the spectral density.

VSD is a general purpose program which uses a Fourier analysis technique to calculate the spectral density of a signal. Before taking a Fourier Transform of the data signal, the program first multiplies the signal by a trapezoidal window in order to reduce leakage. The Fourier Transform is then taken and the periodogram resulting from this operation is smoothed using a simple moving average filter to provide the spectral density function. The length of this filter is set to obtain either a specified filter band width or a specified number of degrees of freedom per spectral estimate. In this project 100 degrees of freedom were specified in order to obtain a smooth spectral density function. Output from the VSD program consists of the spectral density function as well as many spectral parameters including the peak frequency and the zeroth moment of the spectrum.

Portions of the water surface elevation signals of length 5 minutes were analysed using the VSD program. The incident spectral density was obtained by analysing the water surface signals from the tests without the breakwater in place. Signals from three probes were analysed and the incident spectrum was taken as the average of the three measured spectra. The probes labelled "1" "2", and "3" in Figure 2.6 were used and the probe array was located in the same positions used for the

regular wave tests, as is indicated in Figures 2.3 and 2.4. To obtain the reflected spectral density for each test, the water surface elevation signals without the breakwater in place were subtracted from the signals measured with the breakwater in place. This operation provides the reflected water surface elevation signal directly, provided that the incident and reflected wave trains can be assumed to be combined by linear superposition. Program VSD was run on the reflected wave signals obtained in this manner from the three wave probes to get an average reflected wave spectrum. Dividing the reflected by the incident wave spectra provided the reflection coefficient as a function of frequency for each test.

3.3 Analysis of Wave Directionality

In order to examine the multi-directional tests, the directional spectra of the incident and reflected wave fields were estimated using the GEDAP program MLMWP.

The directional spectrum of a wave field can be calculated from measurements of water surface elevations at a number of locations, or from the water surface elevation and water surface slope or horizontal water particle velocities. Program MLMWP read water surface elevation signals measured at five probes and used a maximum likelihood method to calculate the directional spectrum. The maximum likelihood method, MLM provides an estimate of the directional spectrum which maximises the likelihood of obtaining the observed data set. The MLM was described in further detail by Nwogu (1989). Another directional analysis program MLMVL was used to check the results of the MLMWP program. The GEDAP program MLMVL is different from the program MLMWP in that it analyses a water surface elevation signal and horizontal water particle velocity signals rather than five water surface elevation signals.

The directional spectra for the incident and reflected wave fields were obtained using a similar procedure to that used to obtain the spectral density functions. To get the reflected directional spectrum for each test the program MLMWP was applied to the signal resulting from the subtraction of the incident from the combined incident and reflected wave signals. The incident

directional spectrum was obtained by applying MLMWP directly to the incident wave measurements, i.e, measurements made without the breakwater in place.

Chapter 4

RESULTS AND DISCUSSION

4.1 General Observations

The generation of the entire programme of test waves in the open basin before the placement of the breakwater allowed the incident wave field to be examined in the absence of any reflections from the breakwater. This period of testing showed that the incident wave profiles were of satisfactory quality. The incident wave heights were measured and checked against those specified. During the tests without the breakwater in place, the probes were located in positions identical to those used with the breakwater in place. A sample of the measured water surface elevation signals is given in Figure 4.1 showing signals from tests with and without the breakwater in place. This

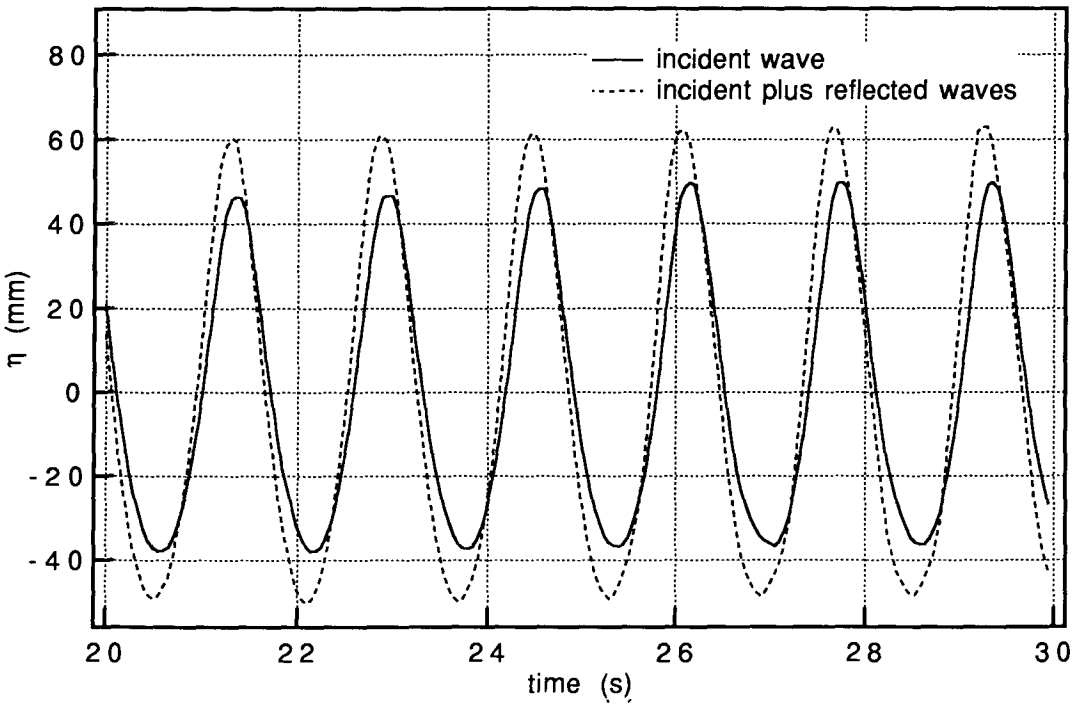

Figure 4.1 - Sample of water surface elevation for test 3 (T = 1.6 s, H = 10 cm) and θ = 45 °, with and without the breakwater in place

figure shows that the combined incident and reflected wave signal is cyclic with the same frequency as the incident signal. No other frequencies are present in the reflected signal indicating that the assumption made in equation (2.1), that there is no scattering of frequency in the reflection process, is valid.

At each wave probe slight variation in incident wave height was observed with time over the seven minute record length. This was attributed to a gradual build up of reflected wave energy from the wave absorbers around the basin sides and also to possible basin resonance. Basin resonance can be encountered when regular waves are generated in a wave basin and it is accepted as being more prominent in regular rather than irregular wave tests. The regular wave analysis was carried out using an initial portion of the record, which was measured before undesired extra reflected wave energy and resonance effects built up, in order to avoid contamination of the results.

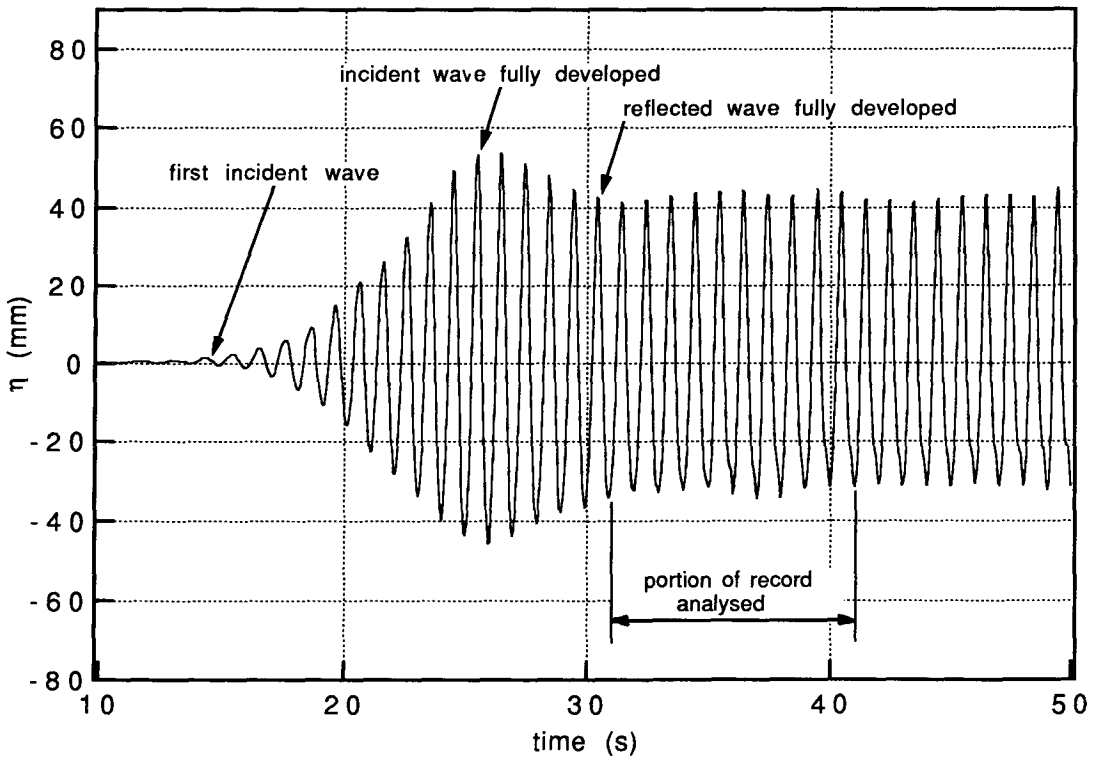

Figure 4.2 - Sample of beginning of wave record showing portion selected for analysis, test 3 (H = 10 cm, T = 1.6 s), θ = 60°

The propogation of the waves across the basin and away from the breakwater needed to be examined in order to ensure that the selected portion contained the fully developed reflected wave from the breakwater as well as the incident wave. Travel times for the wave to travel to the breakwater and to reflect back to the probe array were calculated from the wave group celerity for each different wave type. A 10 second long portion of record, beginning at the instant that the fully developed reflected wave first reached the probe array, was then selected for the analysis of each test. Figure 4.2 shows a 40 second sample of the water surface elevation record for one test including the 10 second portion selected for analysis. The first incident wave was calculated from the wave group celerity to arrive at the probe position at t = 16 seconds, the fully developed incident wave and the fully developed reflected waves were calculated to arrive at t = 26 and t = 31 seconds respectively. Figure 4.2 shows these predictions to be accurate. The addition of the reflected wave, at t = 26 to t = 31 seconds, decreased the amplitude of the total wave signal, which indicates that this probe must have been located near a node in the partial standing wave pattern.

More significant variation in incident wave height was recorded between different wave orthogonals. Spatial variation in wave height was expected in this wave basin due to diffraction and reflection of the generated wave. Such variations were measured in this basin by Shaver (1989) and wave height variations in the basin can also be predicted using a linear diffraction model. In this project the unwanted diffraction of the incident wave was reduced with the use of guidewalls, however some variation was still observed. Differences in incident wave height between the wave probe array and the incident wave probe of up to ten percent were recorded. Differences were generally less than 5 percent and allowance was made for this in the reflection analysis, as described in the previous section, so that the results would not be affected.

4.1.1 Wave-Breakwater Interaction

Due to the principle of conservation of energy, the sum of the energy reflected from, transmitted through, and dissipated by the breakwater must be equal to the total wave energy incident upon the

breakwater. Therefore, the amount of wave reflection is directly affected by the amounts of wave transmission and wave energy dissipation.

Wave transmission was observed to be negligible in this project. Wave energy dissipation due to wave-breakwater interaction was observed in the form of wave breaking and run-up on the structure. Very different wave-breakwater interactions were observed for the range of waves tested. Longer period waves appeared to lose less energy in turbulence when they broke on the breakwater when compared to the steeper short period waves. Also, waves with more oblique angles of incidence tended to show less vigorous action on the breakwater face.

4.2 Regular, Uni-Directional Wave Tests

4.2.1 Performance of Sinusoidal Fitting Program

The performance of the curve fitting program APHRES, which fitted sinusoidal curves to the 10 second portions of water surface signal for each test, was checked visually by plotting the sinusoidal curve superimposed on the measured signal. Samples of these plots are shown in Figures 4.3 to 4.5. From these plots it can be seen that there is no perceptible difference in phase between the measured and fitted signals, but that there is some difference between the amplitudes of the two signals. Also shown on each of the plots is the difference between the measured water surface elevation and that given by the fitted curve. In these figures the mean of the difference signal is not equal to zero, implying that the wave probes were not zeroed before this test and hence the mean of the measured signal is not zero. These difference curves are observed to consist mainly of the second harmonic to the fundamental wave.

Second harmonic wave activity is commonly encountered when regular waves are generated in a wave basin or flume and is made up of two main components:

1) One component of second harmonic waves is bounded to the fundamental wave train, and will exist in all except deep water conditions. This component

propogates at the same celerity as the fundamental wave train and gives the wave a non-linear profile.

2) Another component of second harmonic wave activity may be present depending on the wave generation method used. Most wave generation techniques, including the method used in this study, use first order theory to calculate paddle motions. This theory does not satisfy the necessary second order boundary conditions and therefore undesired free waves of frequency twice that of the fundamental are produced. These propogate at a different speed to that of the fundamental wave train and so will lead to different wave profiles at different locations.

Another component of second harmonic wave activity may be present due to the wave reflection process. When a portion of the fundamental wave train is reflected from the breakwater a certain amount of bounded second harmonic wave must also be present in the reflected wave for it to retain its non-linear profile. Any excess in reflected second harmonic wave energy over this amount will be released as free second harmonic wave activity. Higher harmonic activity was not of interest in this study and therefore no analysis of these components was undertaken. A more generous treatment of the reflection of second harmonic waves is given by Mansard et al. (1985).

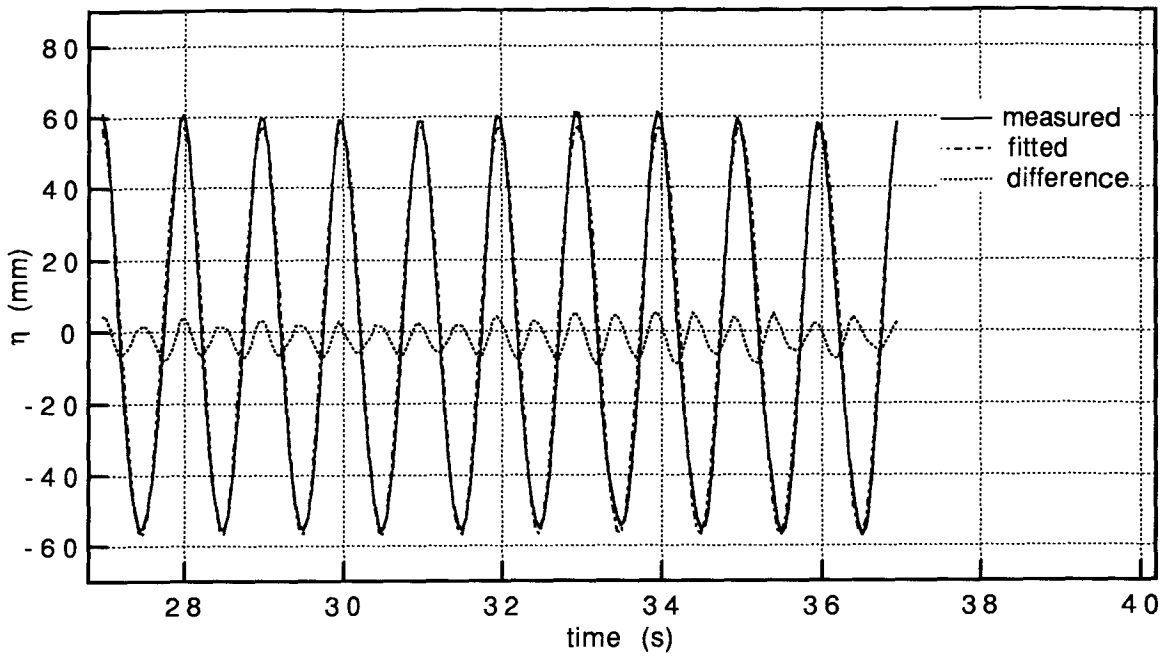

Figure 4.3 - Results of the sinusoidal fitting program APHRES, test 1 (H = 10 cm, T = 1.0 s), θ = 45°

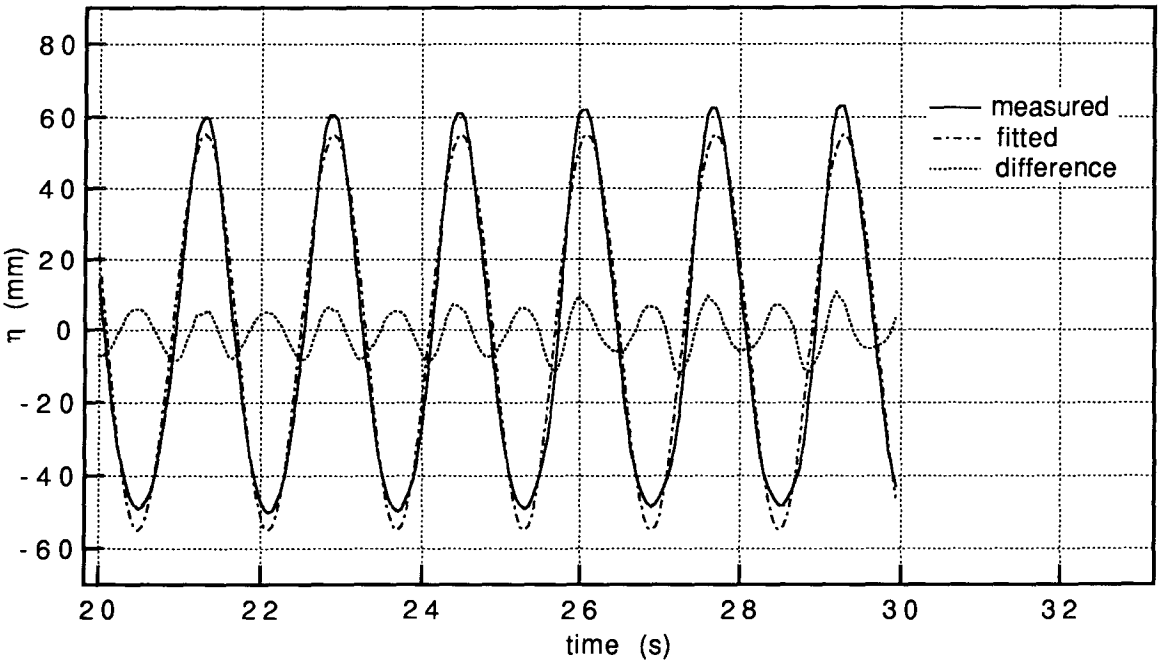

Figure 4.4 - Results of the sinusoidal fitting program APHRES, test 3 (H = 10 cm, T = 1.6 s), θ = 45°

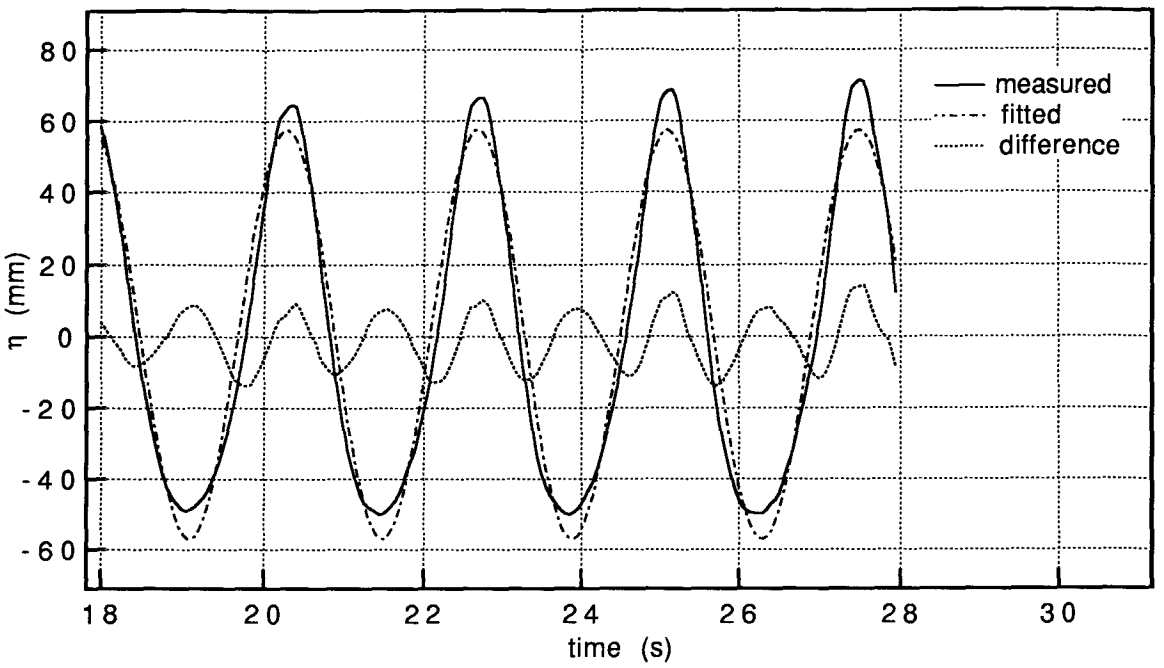

Figure 4.5 - Results of the sinusoidal fitting program APHRES, test 5 (H = 10 cm, T = 2.4 s), θ = 45°

4.2.2 Accuracy of the Least Squares Method

As a test of the accuracy of the least squares method, incident wave amplitudes derived from analysis of wave records measured with the breakwater in place were compared to incident amplitudes measured without the breakwater in place. In general, good accuracy was obtained, with a maximum error of 8% of the measured amplitude and an average error for all the tests of 3%.

A further check on this method of analysis was made by analysing data from the normal incidence tests with a computer program based directly on Mansard and Funke's least squares method rather than the method used in this project. Comparison of the results from the two methods showed that the reflection coefficients obtained by the two methods agreed to within one percent accuracy, although this is generally expected since the present method is essentially a variant of that given by Mansard and Funke.

4.2.3 Reflection Coefficient

The most important parameter describing wave reflection is the reflection coefficient, K_r. Results from the analysis showed that for the entire range of wave types tested, and for all the angles of incidence, K_r ranged from 10% to 59%. The highest reflection coefficient of 59% was recorded for a wave height of 10 *cm* and period of 2.4 *s* with angle of incidence of 30°.

The dimensional analysis in Equation (2.2) indicates that for a given breakwater and water depth and for regular, uni-directional incident waves, the reflection coefficient K_r and phase angle β each depend on the three parameters, the wave steepness H/L, the depth to wave length ratio d/gT^2 and the incident direction θ.

The dependence of K_r on H/L is shown in Figure 4.6, in which K_r is plotted as a function of H/L for a constant value of $d/gT^2 = 0.020$ and with $\theta = 0°$ and 45° in turn. The reflection coefficient K_r is seen to decrease very slightly with increasing wave height, such that K_r varies from 10% to 14% for $\theta = 0°$ and from 32% to 39% for $\theta = 45°$ over the range of wave heights encountered. This small variation indicates that K_r has a very slight dependence on wave height and suggests that the depth to wave length ratio d/gT^2 and the angle of incidence θ may be more important.

Figures 4.7 to 4.10 show K_r plotted against d/gT^2 for each angle of wave incidence. In the figures, values of H/L vary from 0.014 to 0.073, however this is not expected to have much influence on the relationships on account of the observations taken from Figure 4.6. As expected, K_r was found to decrease with increasing wavelength parameter, that is, with decreasing wavelength. For angles of incidence $\theta = 0°$ and 30° K_r decreased dramatically as d/gT^2 increased from 0.01 to 0.02. However, there was no further decrease in K_r as d/gT^2 was increased further from 0.02 to 0.05, instead K_r remained approximately constant at values of $K_r = 0.15$ and 0.23 for $\theta = 0°$ and 30° respectively. This plateau in the K_r versus d/gT^2 relationship may be associated with a maximum level in the proportion of energy able to be dissipated by the breakwater. As d/gT^2 is increased from 0.01 to 0.02 the proportion of wave energy dissipated by the breakwater

increases as the wave breaking on the structure becomes more vigorous. It is expected that, due to the principal of conservation of energy, the amount of energy reflected from the breakwater must therefore decrease as d/gT^2 is increased, as is shown by Figures 4.7 to 4.10. At a value of d/gT^2 of 0.02, where the proportion of incident wave energy dissipated is approaching unity, this proportion is observed to reach a maximum as K_r decreases no further. This abrupt change in wave reflection is probably associated with a transition in the type of wave breaking on the structure from a surging type of wave, with low energy dissipation characteristics, to a plunging type of wave, with high energy dissipation characteristics and a low reflection coefficient. This speculative proposition may be used to explain the disjoint shapes of the curves in Figures 4.7 and 4.8. For angles of incidence of $\theta = 45°$ and 60°, because the waves are approaching at an oblique angle, which means that at different positions along each wave crest the waves are at various stages of breaking, a different transition between the types of wave breaking can be expected. For higher angles of incidence the relationship between K_r and d/gT^2 can therefore be expected to change to a less disjoint, more continuous function, as is shown by Figures 4.9 and 4.10.

Figure 4.11 combines the results shown in Figures 4.7 to 4.10 and emphasizes the effect of angle of incidence on the reflection coefficient over the range of wavelength parameter d/gT^2 examined. In Figure 4.12 K_r is plotted against angle of incidence θ for intermediate and larger values of d/gT^2. Figures 4.12 shows that the plateau in K_r observed in Figures 4.7 to 4.10 occurs at values of K_r that increase significantly with increasing angle of incidence. This indicates that as θ increases, the consequent decreasing vigour of the wave action on the breakwater that was observed in Section 4.1.1 leads to a decrease in the proportion of energy dissipated by the breakwater and therefore an increase in the minimum value of K_r. For the smaller values of d/gT^2, Figure 4.13 shows that the effect of θ on K_r is different and that the largest values of K_r were measured for $\theta = 30°$.

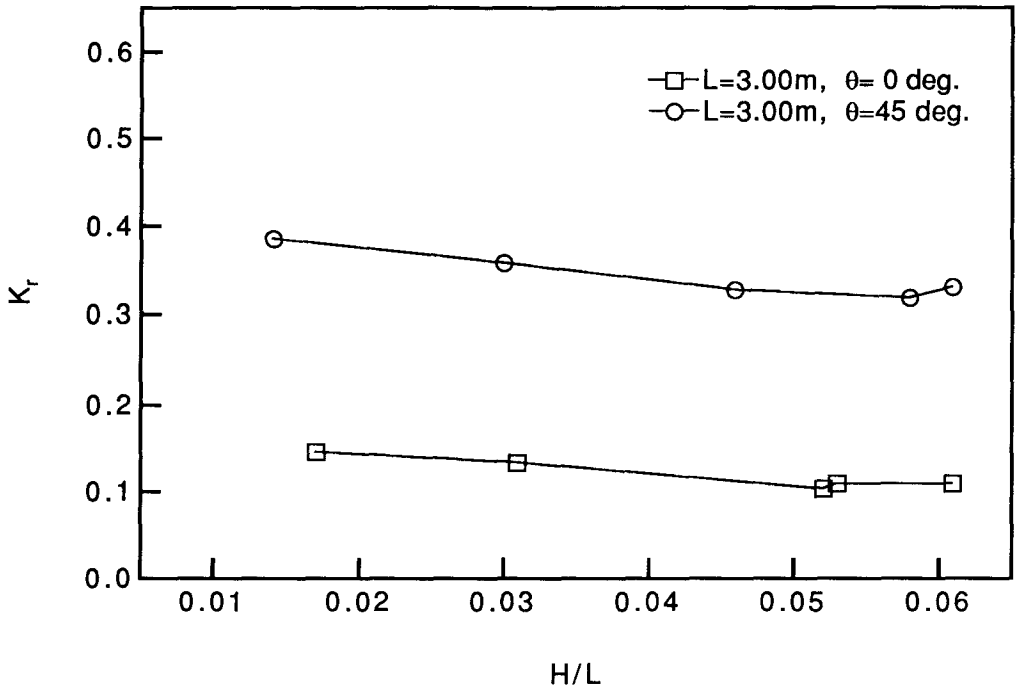

Figure 4.6 - Reflection coefficient vs. wave steepness, $d/gT^2 = 0.020$, $\theta = 0°, 45°$

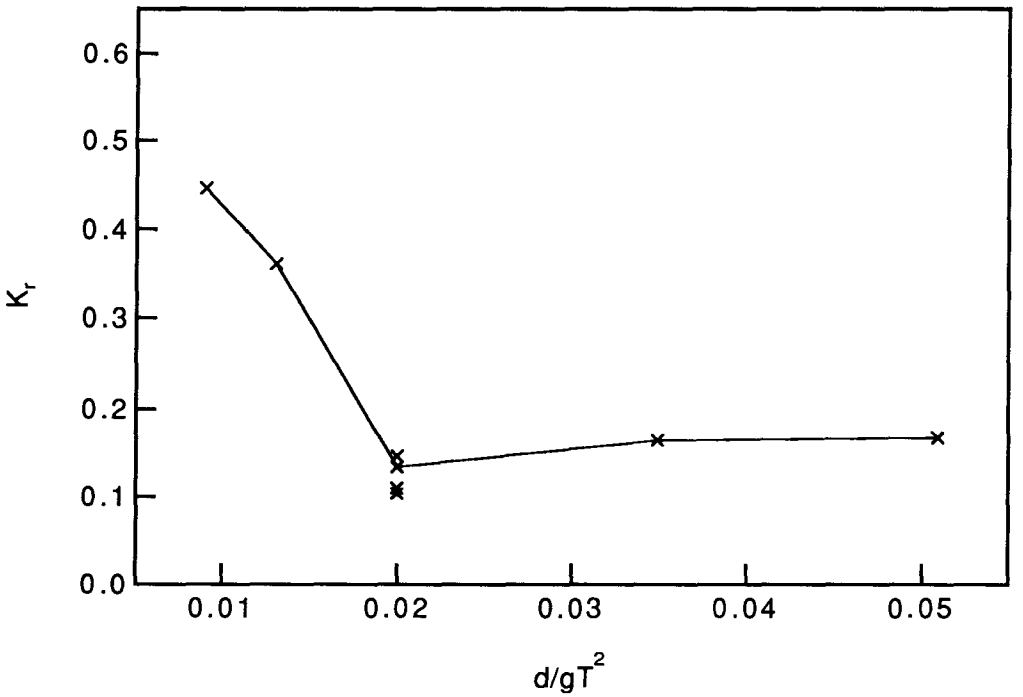

Figure 4.7 - Reflection coefficient vs. d/gT^2, $\theta = 0°$

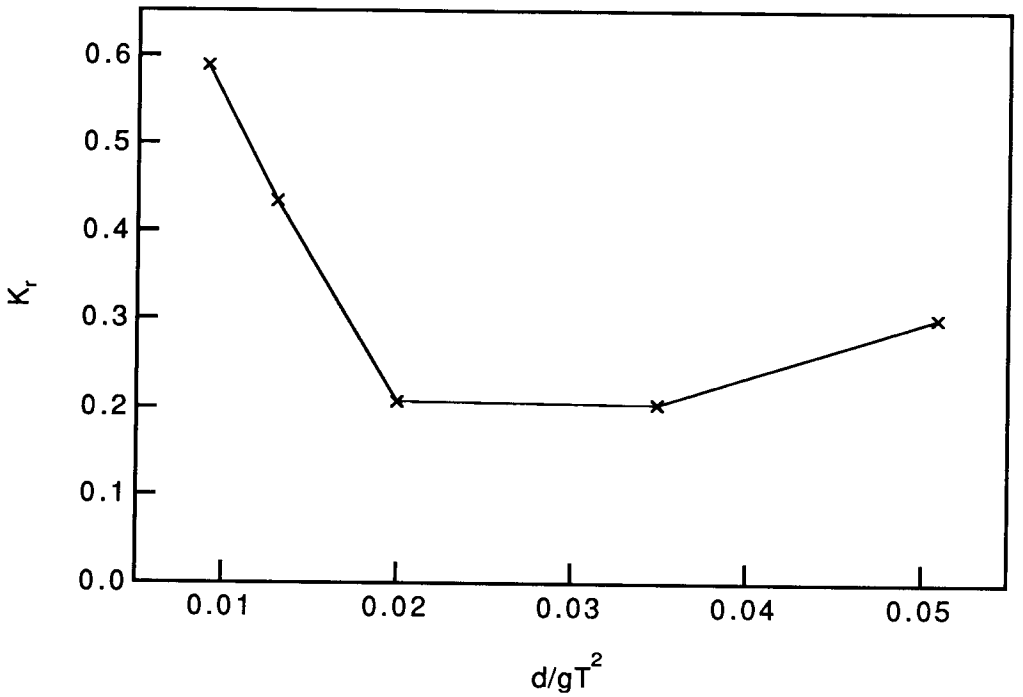

Figure 4.8 - Reflection coefficient vs. d/gT^2, $\theta = 30°$

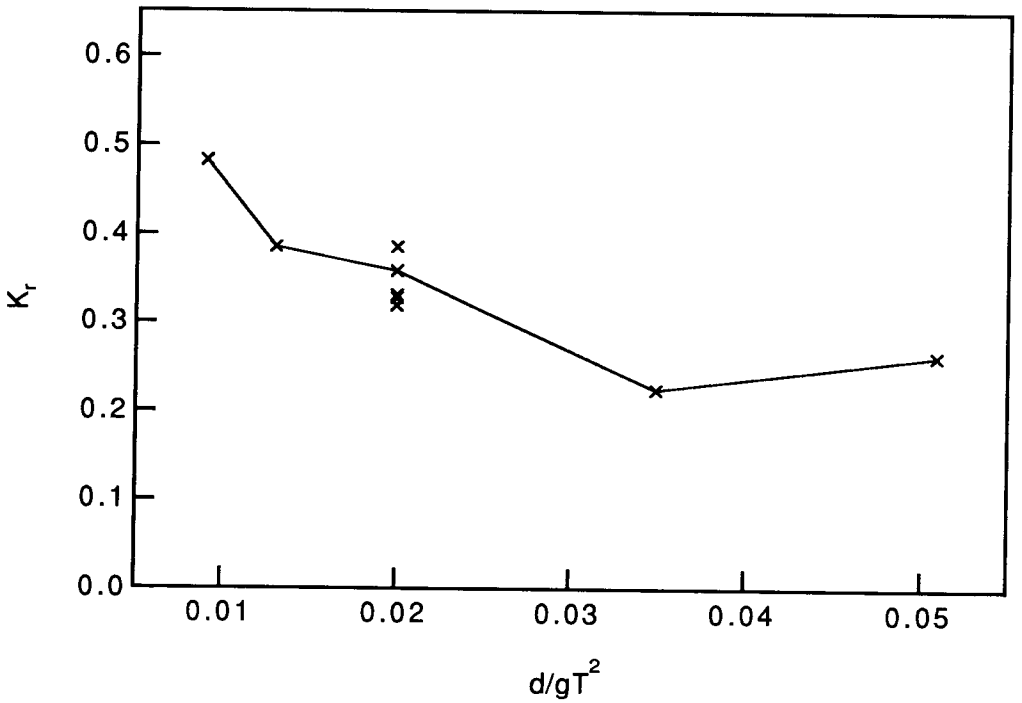

Figure 4.9 - Reflection coefficient vs. d/gT^2, $\theta = 45°$

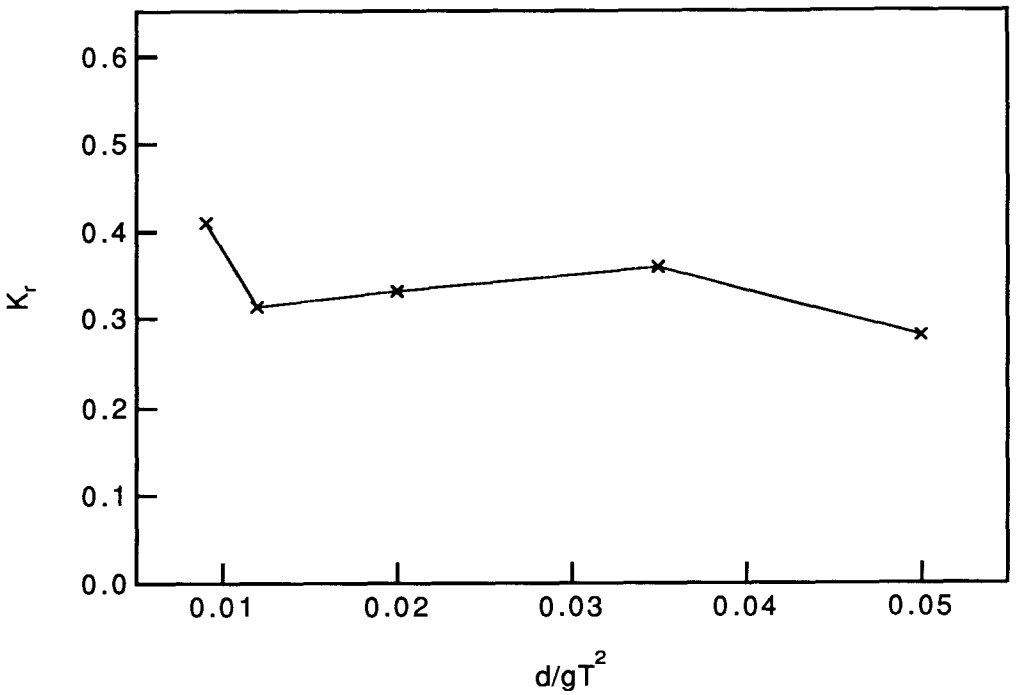

Figure 4.10 - Reflection coefficient vs. d/gT^2, $\theta = 60°$

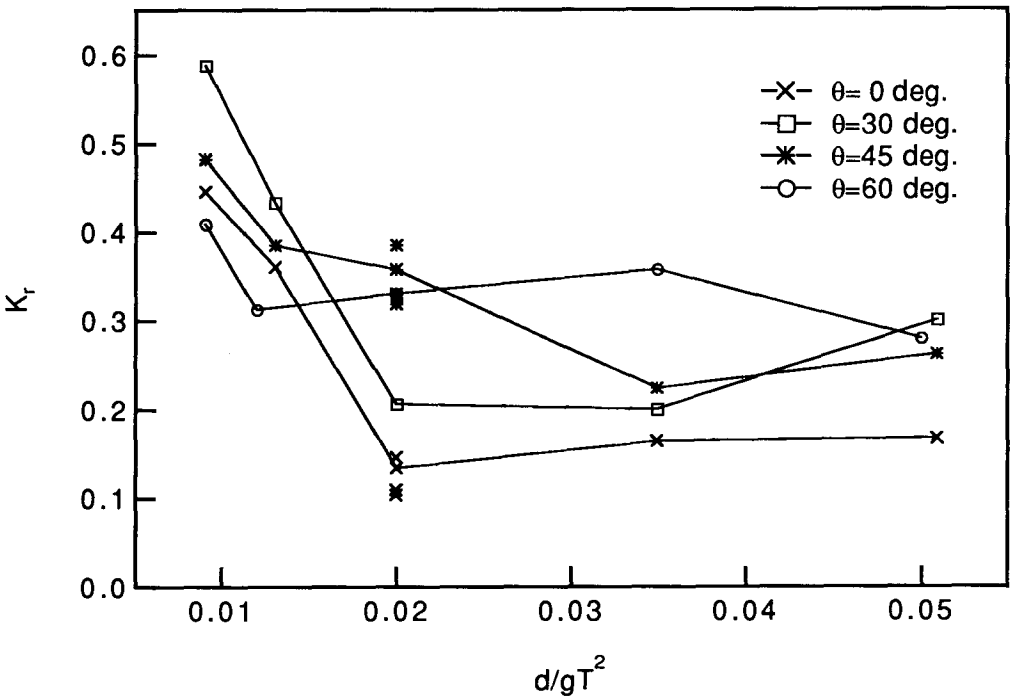

Figure 4.11 - Reflection coefficient vs. d/gT^2

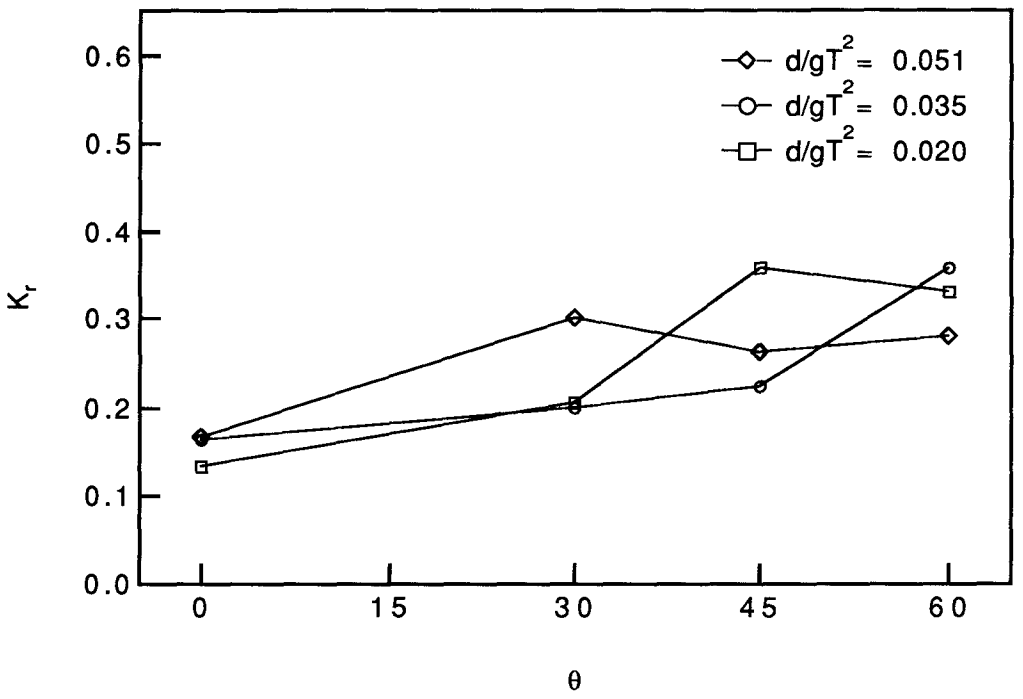

Figure 4.12 - Reflection coefficient vs. angle of incidence, high d/gT^2

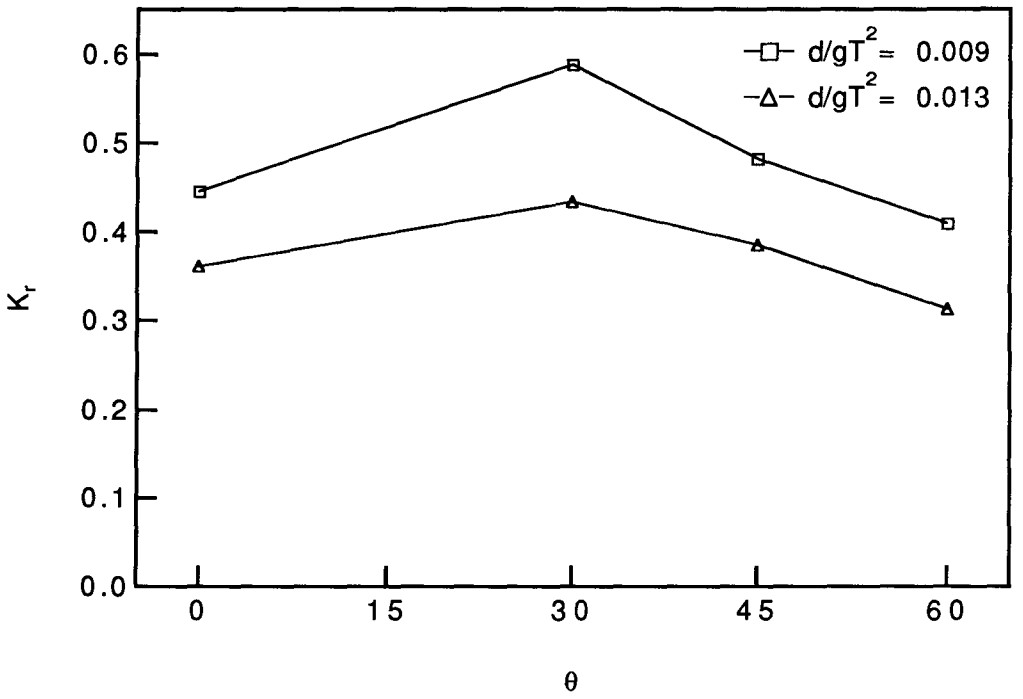

Figure 4.13 - Reflection coefficient vs. angle of incidence, low d/gT^2

4.2.4 Reflected Phase Lag

The reflected phase lag β is the reflection characteristic which determines the lateral shift of the partial standing wave pattern from the reflecting boundary. $\beta = 0°$ corresponds to anti-nodes at integer half wavelengths from the origin of the x axis. If $\beta > 0°$ then this standing wave pattern is shifted in a direction towards the breakwater. Results of this study gave β as well as the more important wave reflection variable K_r. These results showed that β can be as large as one quarter of a cycle. For the entire range of regular wave tests β ranged from 9° to 116°.

From Equation (24), and using the notation defined in Figure 4.14, it can be shown that the relationship between β and the shift in the standing wave position x' is:

$$x' = \frac{\beta}{2k} = \frac{\beta}{4\pi} L \qquad (4.1)$$

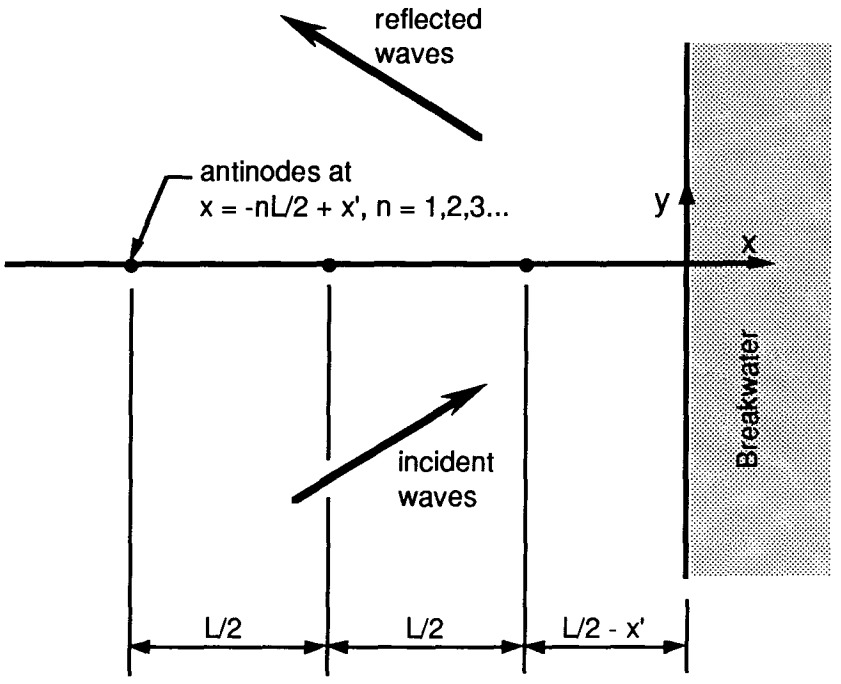

Figure 4.14 - Sketch showing effect of phase lag on partial standing wave position

In similar manner to the reflection coefficient analysis, analysis of the reflected phase lag was carried out to examine relationships between β and the parameters describing the wave characteristics, the wave steepness H/L, the depth to wavelength ratio d/gT^2, and the angle of incidence θ.

The dependency of β on the wave steepness is seen in Figure 4.15. In this figure β is plotted against wave steepness H/L for constant values of d/gT^2, and $d = 0.5\ m$, $d/gT^2 = 0.020$ and $\theta = 0°$ and 45° in turn. From this plot it is seen that β has only a very small dependence on wave height, as was found for the relationship between K_r and wave height.

Figures 4.16 to 4.19, in which β is plotted against d/gT^2 for each angle of incidence in turn, show that β has a strong dependency on d/gT^2. These plots indicate that β increases with increasing d/gT^2, i.e: decreasing wavelength. However, for $\theta = 60°$, β is seen to be independent of d/gT^2. This difference in the behaviour of β may be due to to the fact that the angle of incidence of $\theta = 60°$ is very extreme. The results shown in Figures 4.16 to 4.19 are combined in Figure 4.20, in which β is plotted against d/gT^2 for all angles of incidence. This plot shows that β is also dependent on angle of incidence θ, and indicates that β increases with increasing θ. The dependency of β on d/gT^2 may be explained by examining the shift in position of the standing wave pattern x', given by Equation (4.1). Figure 4.21, in which x' is plotted against d/gT^2 for all angles of incidence, shows that for all angles of incidence except $\theta = 60°$, x' is approximately constant. Therefore, from Equation (4.1), β must increase with increasing d/gT^2.

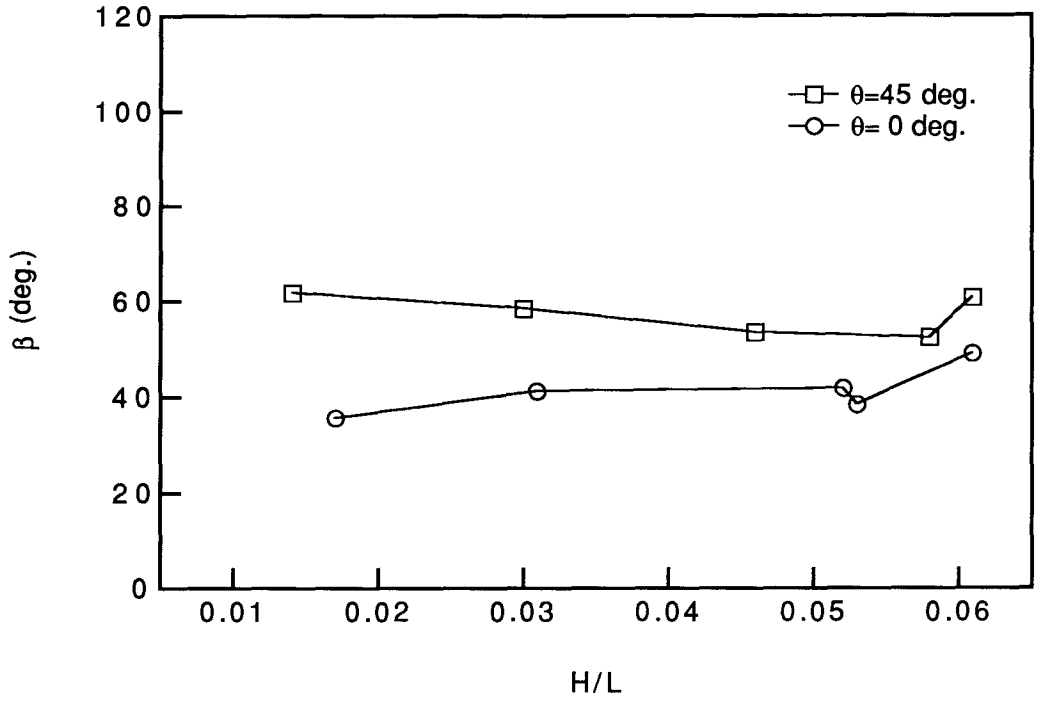

Figure 4.15 - Reflected phase lag vs. wave steepness, $d/gT^2 = 0.020$, $\theta = 0°, 45°$

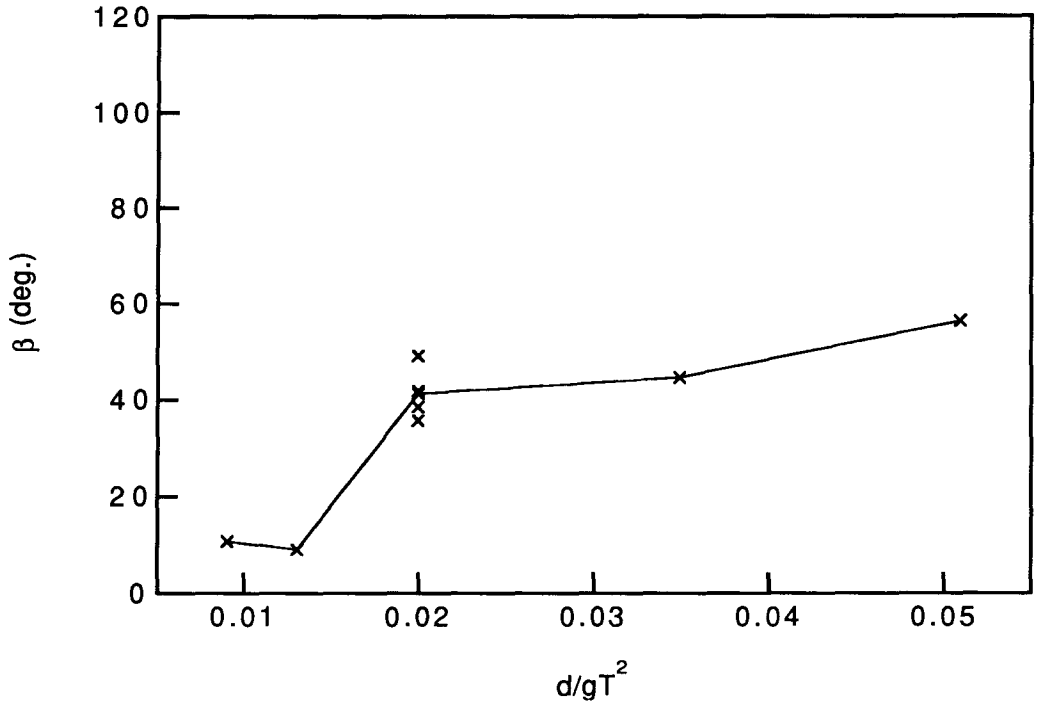

Figure 4.16 - Reflected phase lag vs. d/gT^2, $\theta = 0°$

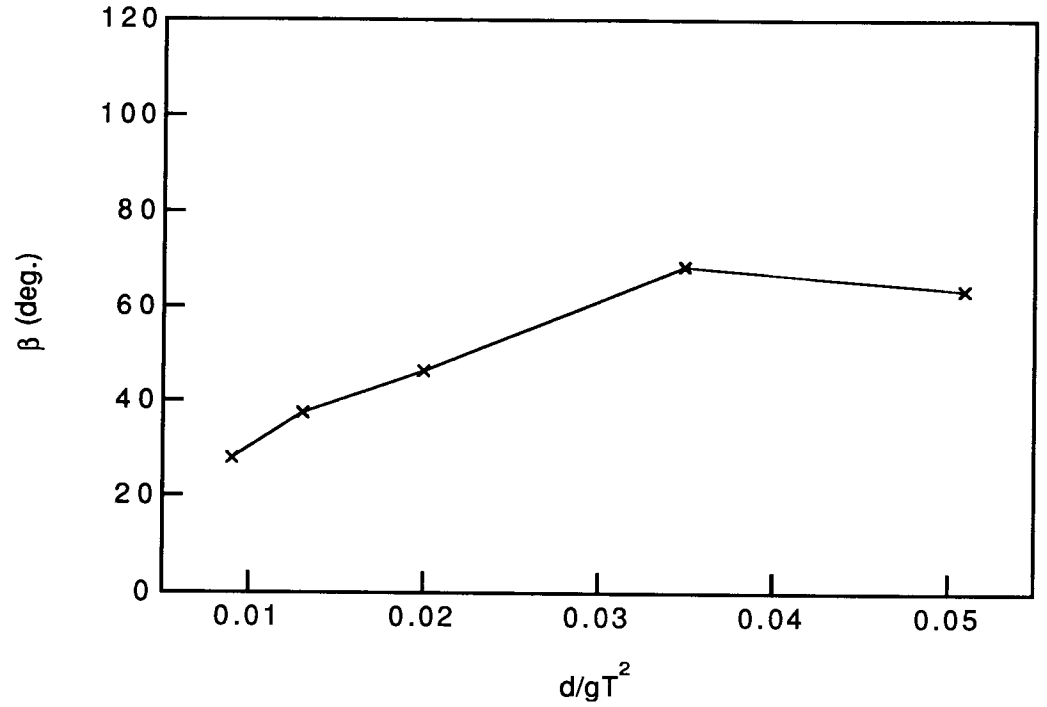

Figure 4.17 - Reflected phase lag vs. d/gT^2, $\theta = 30°$

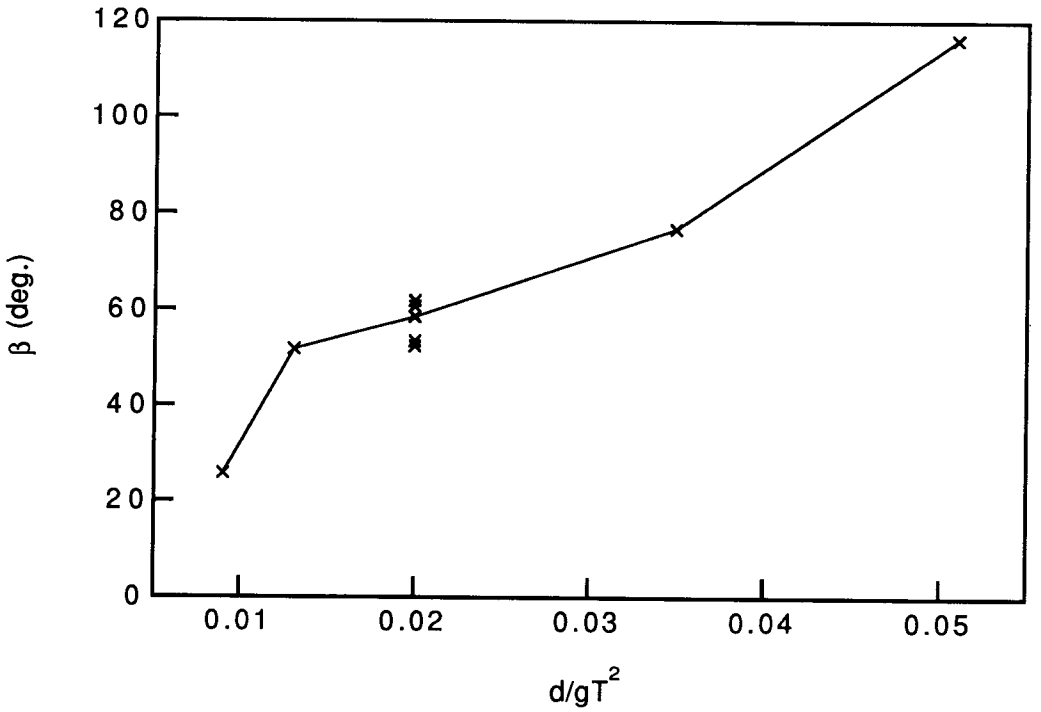

Figure 4.18 - Reflected phase lag vs. d/gT^2, $\theta = 45°$

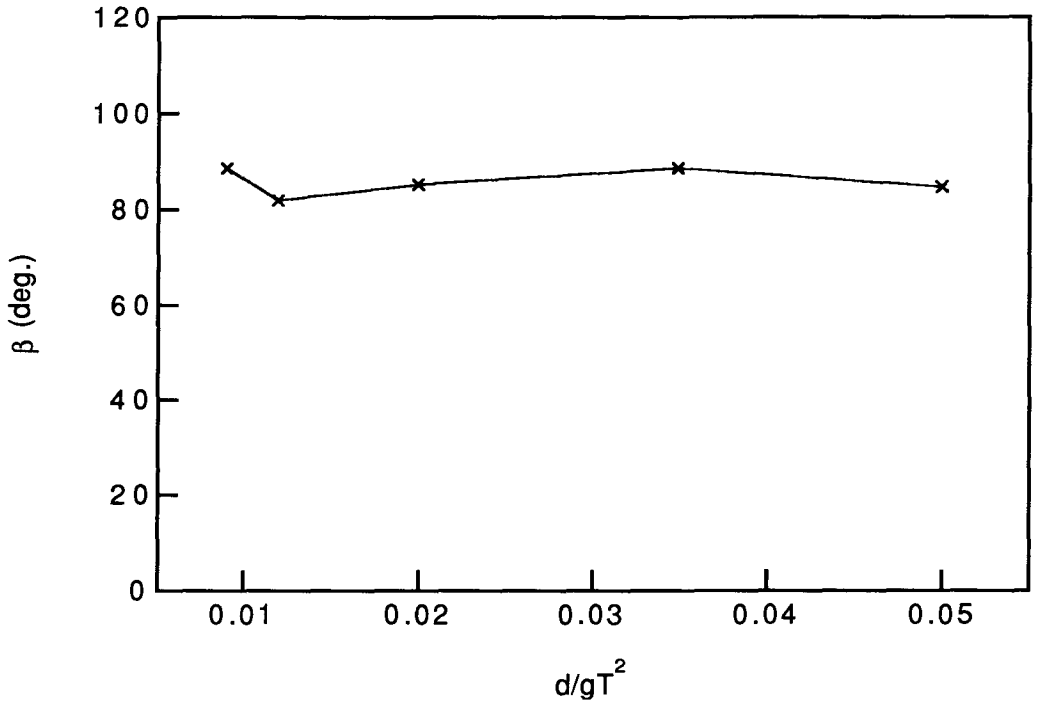

Figure 4.19 - Reflected phase lag vs. d/gT^2, $\theta = 60°$

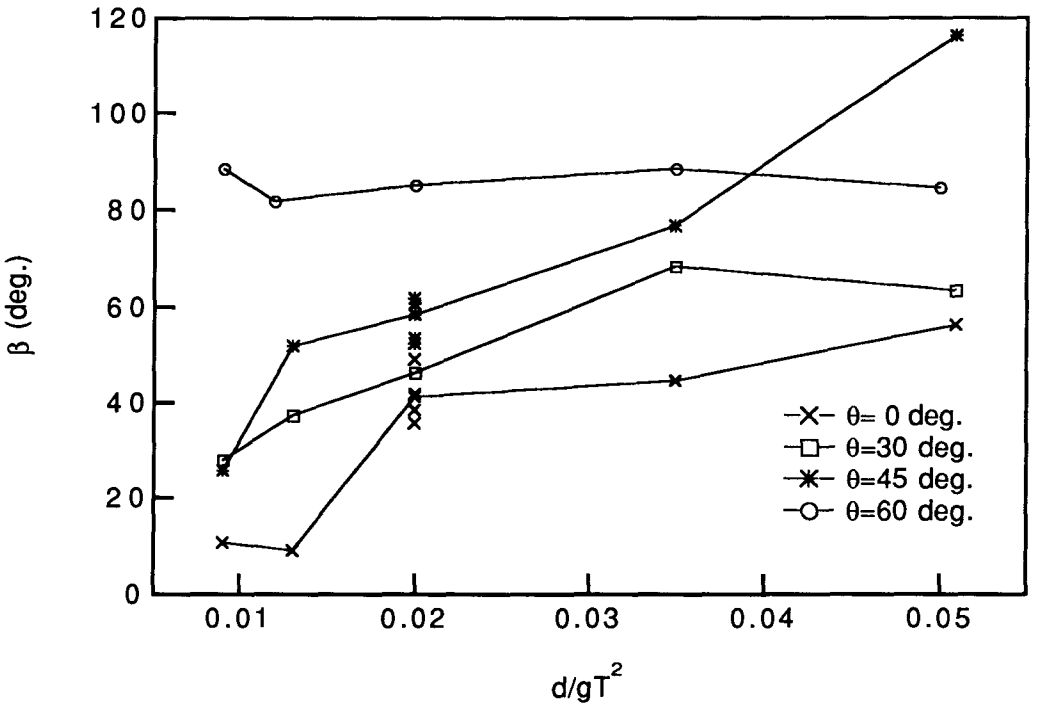

Figure 4.20 - Reflected phase lag vs. d/gT^2

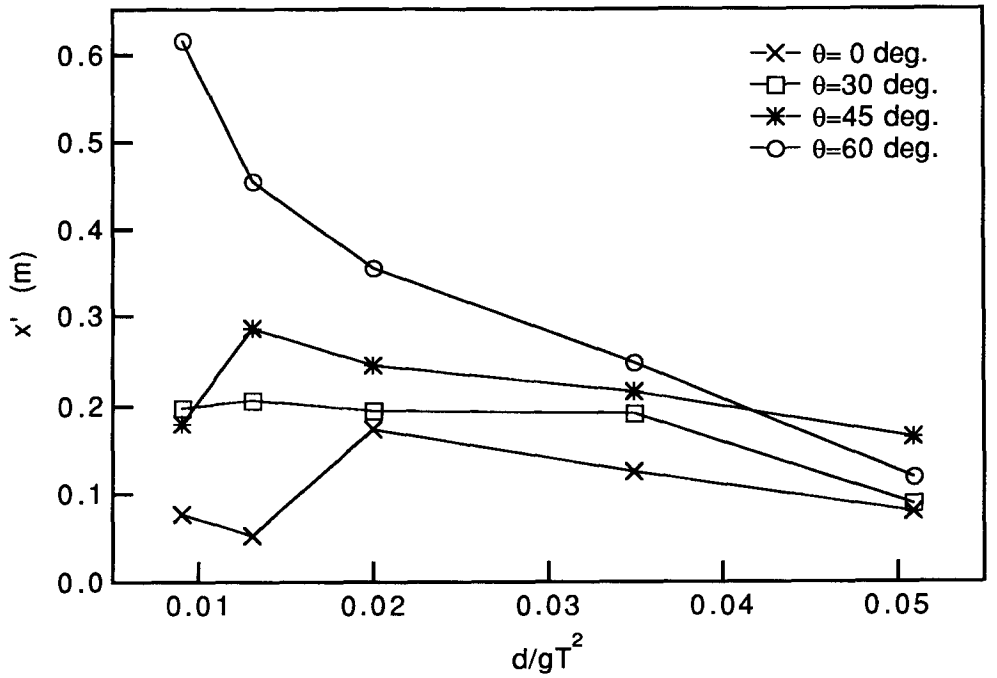

Figure 4.21 - Reflected phase lag vs. d/gT^2

4.3 Irregular Wave Tests

The purpose of the phase of testing with irregular waves was to determine whether the results obtained from the regular reflection tests could be applied accurately to reflection of irregular waves. This has been done by estimating spectral density functions for the incident and reflected wave fields and thereby calculating the reflection coefficient as a function of frequency. This reflection coefficient function can be directly compared to the reflection coefficients for each wave period measured in the regular tests.

4.3.1 Spectral Density Functions

Figures 4.22 to 4.25 show estimates of spectral density for the four particular tests, $T_p = 1.6\ s$, $H_S = 6\ cm$ and $12\ cm$ in turn, and $\theta = 0°$ and $45°$ in turn. The use of program VSD in the analysis meant that smooth frequency spectra were able to be obtained. This smoothing was needed to obtain meaningful results when the reflected spectra were divided by the incident spectra to obtain the reflection coefficient function. From these plots it is apparent that the reflected wave energy is of the same approximate frequency range as the incident wave energy. The reflected frequency spectra do, however, show a disproportionately high amount of reflected wave energy for frequencies in the range $f > 1.5\ Hz$. Also, the peaks of the reflected spectral density appear to be at a lower frequency than the peaks of the incident spectral density. Results from the regular wave tests, indicating that the lower frequency waves would have more energy reflected than the higher frequency waves, also predict this shift in the peak frequency of the reflected wave field.

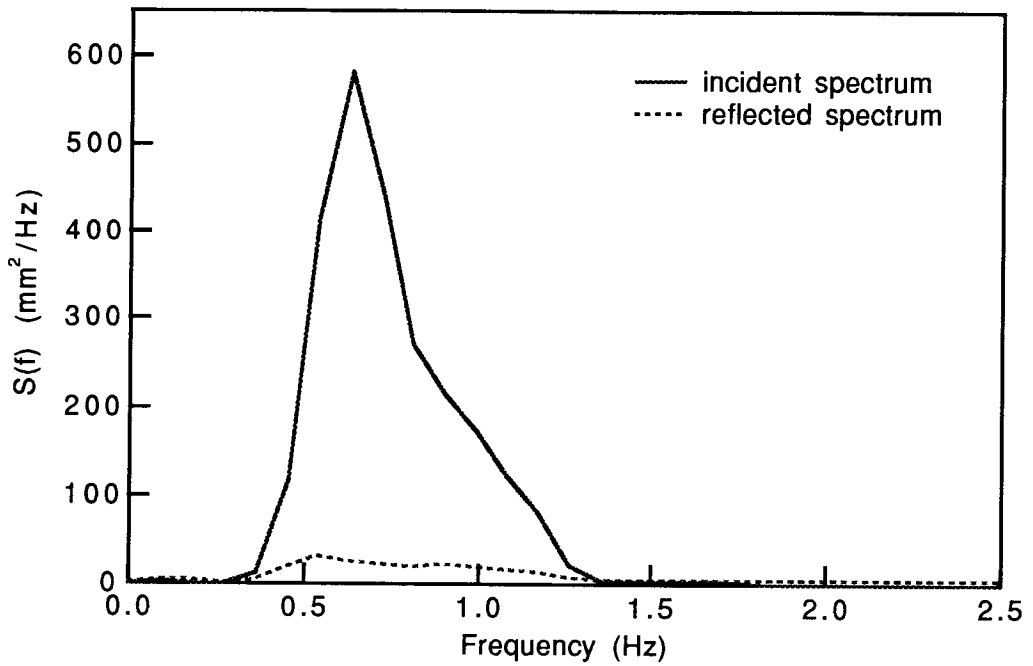

Figure 4.22 - Incident and reflected spectral density, test 10 (H_S = 6 cm, T_P = 1.6 s) and $\theta = 0°$

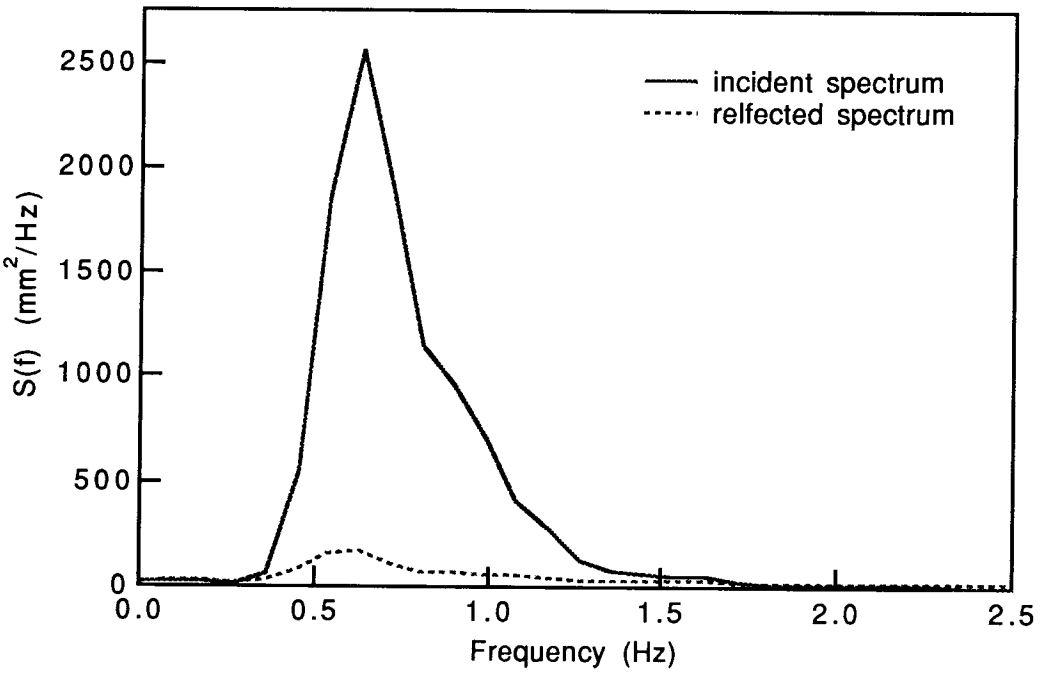

Figure 4.23 - Incident and reflected spectral density, test 11 (H_S = 12 cm, T_P = 1.6 s) and $\theta = 0°$

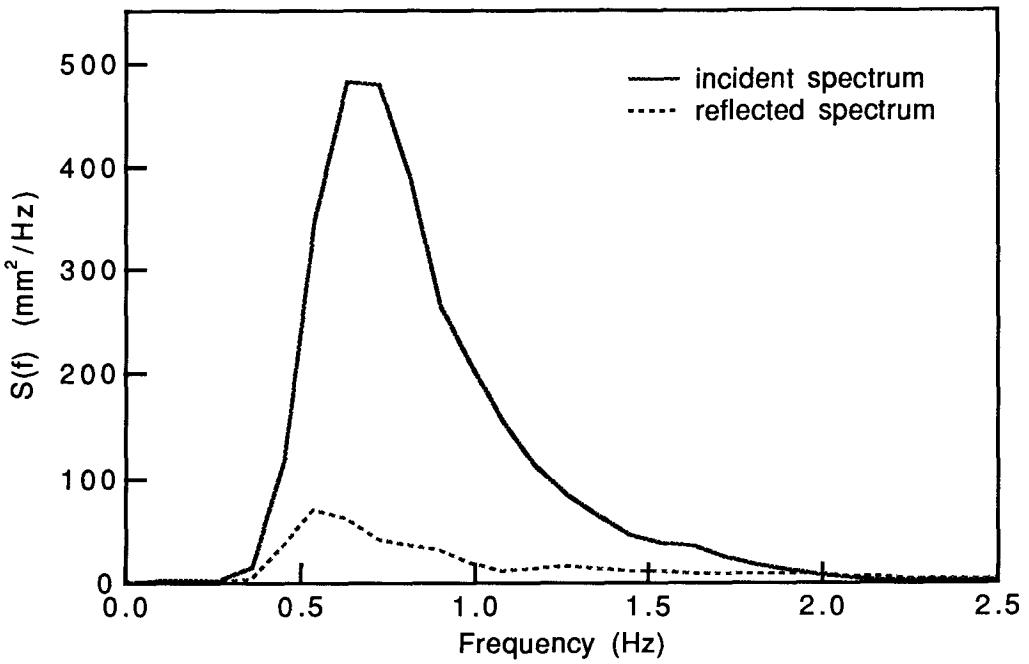

Figure 4.24 - Incident and reflected spectral density, test 10 (H_S = 6 cm, T_P = 1.6 s) and $\theta = 45°$

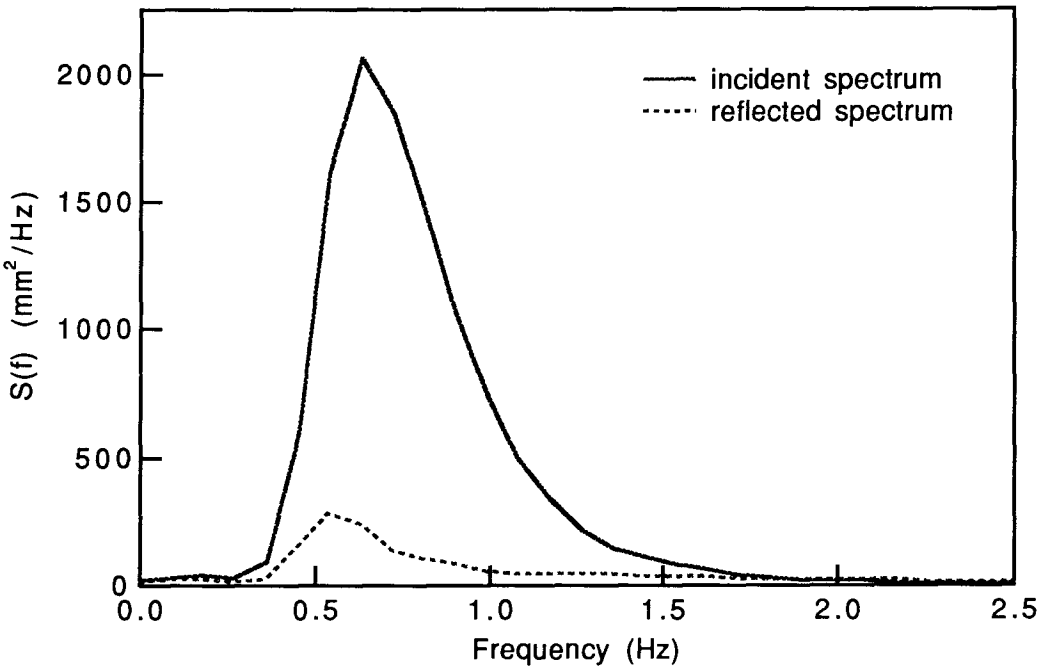

Figure 4.25 - Incident and reflected spectral density, test 11 (H_S = 12 cm, T_P = 1.6 s) and $\theta = 45°$

4.3.2 Comparison of Irregular and Regular Reflection Coefficients

Figures 4.26 to 4.29 show the average reflection coefficients and the reflection coefficients as functions of frequency for the irregular wave tests. These figures show that the estimated reflection coefficient functions for the irregular wave tests exhibit a reasonably close fit to those measured in the regular wave tests.

For $\theta = 0°$, estimated reflection coefficients are higher than those measured in regular tests above a frequency of 0.6 *Hz,* and for frequencies greater than 1.0 or 1.2 *Hz* in all irregular tests, high values of reflection coefficient were measured. This is thought to be due to scattering of wave energy from lower to higher frequencies caused by turbulent wave-breakwater interaction. The result of this action is that wave energy, incident at low frequencies, is reflected at higher frequencies. This is more apparent for the tests with $\theta = 0°$, which indicates that the more vigorous action of the normally incident waves, as observed in Section 4.1.1, has lead to more frequency scattering.

Values of average reflection coefficient $\overline{K_r}$ of 31.2% and 31.5% were measured for $\theta = 0°$ and $H_S = 6$ *cm* and 12 *cm* respectively, and for $\theta = 45°$ the measured values of $\overline{K_r}$ were 39.0% and 37.5% with the same respective significant wave heights. The dependency of $\overline{K_r}$ on θ and H_S can be examined using these results. For the limited number of irregular tests undertaken, it is apparent that $\overline{K_r}$ varies more with θ than with H_S. This is a similar result to that obtained in the regular wave tests, indicating that the average reflection coefficient has very little dependence on the significant wave height, while having a stronger dependency on θ. Higher values of $\overline{K_r}$ were recorded for $\theta = 45°$ in comparison to $\theta = 0°$. This indicates that $\overline{K_r}$ is dependent on θ and that $\overline{K_r}$ increases with increasing θ, as was found for the regular wave tests with high d/gT^2.

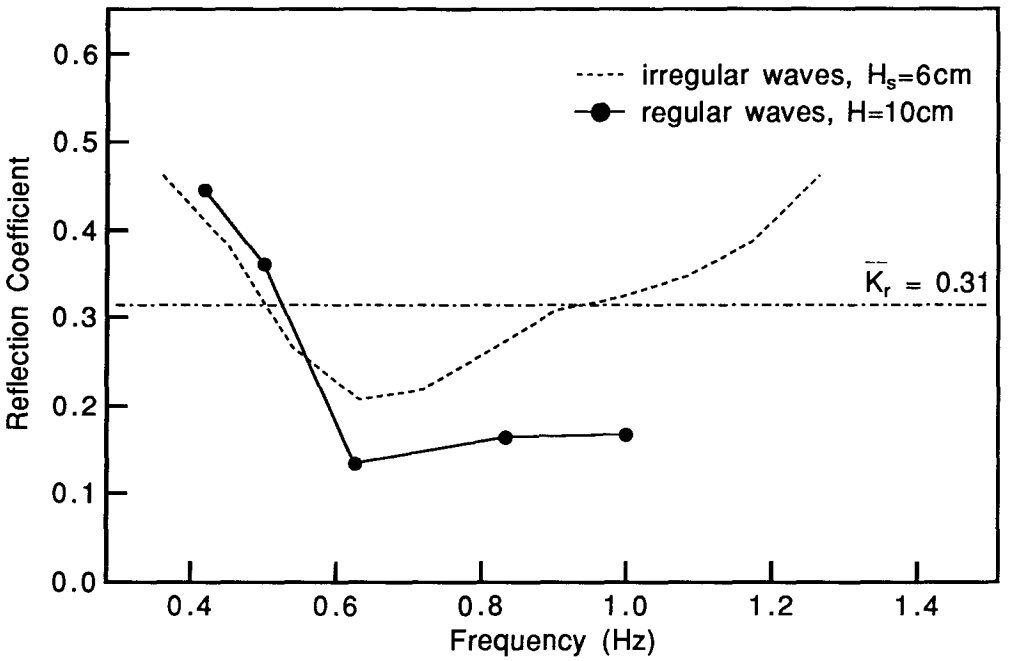

Figure 4.26 - Comparison of regular and irregular reflection coefficients, test 10 (H_S = 6 cm, T_P = 1.6 s) and $\theta = 0°$

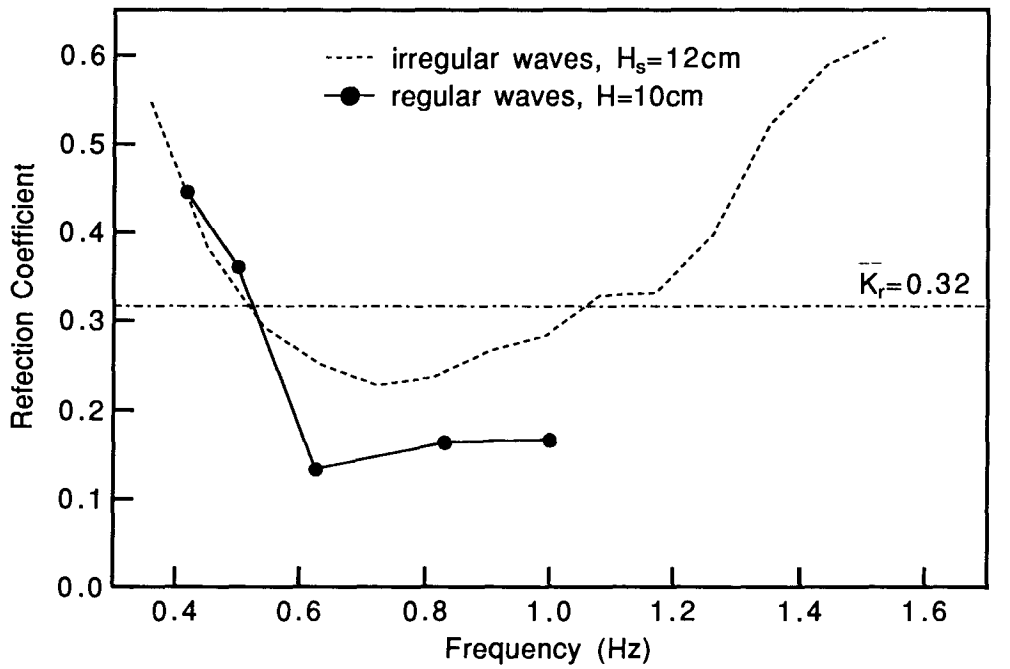

Figure 4.27 - Comparison of regular and irregular reflection coefficients, test 11 (H_S = 12 cm, T_P = 1.6 s) and $\theta = 0°$

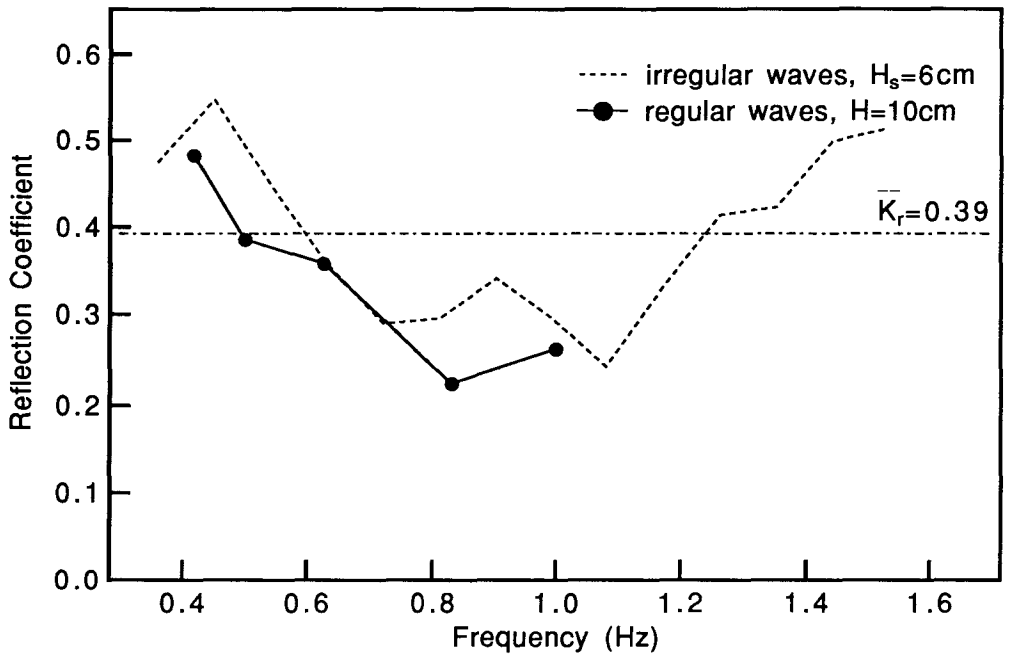

Figure 4.28 - Comparison of regular and irregular reflection coefficients, test 10 (H_S = 6 cm, T_p = 1.6 s) and θ = 45 °

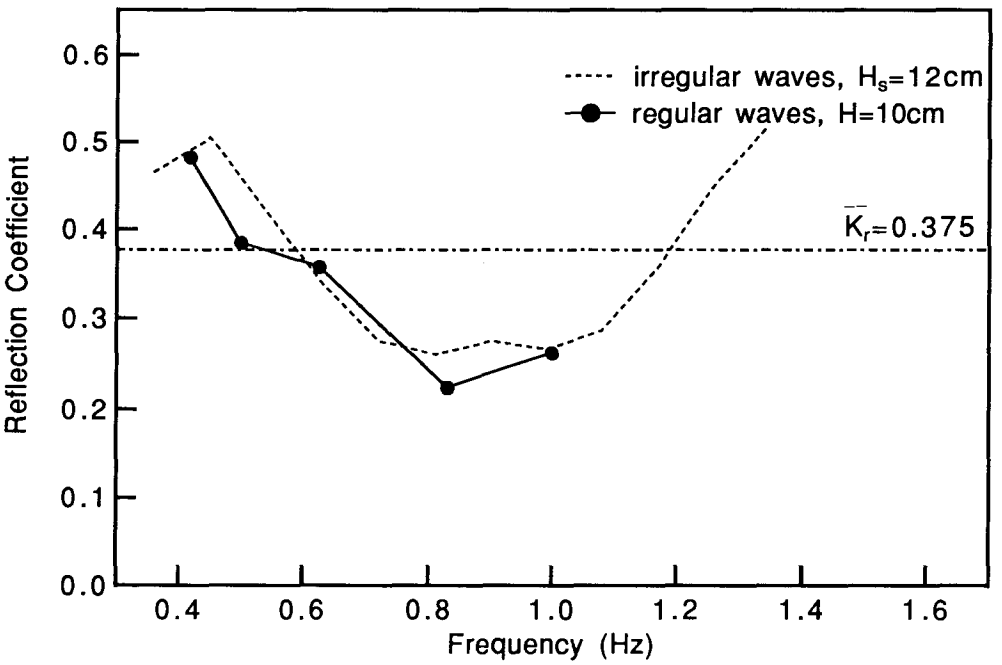

Figure 4.29 - Comparison of regular and irregular reflection coefficients, test 11 (H_S = 12 cm , T_p = 1.6 s) and θ = 45 °

4.4 Directionality Results

The phase of testing with multi-directional waves was undertaken to investigate two characteristics of reflection from the breakwater. These were:

1) The principal direction of the reflected waves and whether the angle of reflection is equal to the angle of incidence.

2) The amount of directional spreading in the reflected wave field.

Tests were analysed using the analysis program MLMWP. This program was developed by the Hydraulics Laboratory and the performance of this program has been described in detail by Nwogu (1989). Further development of the program to make it more suitable for wave fields containing incident and reflected wave energy was considered to be beyond the scope of this study. For this reason, as was previously mentioned, the incident wave field was extracted so that the method could be applied to the reflected wave field alone. However, errors can be introduced in this process when the incident wave signal is subtracted from the combined incident and reflected signal.

Tests were performed with multi-directional waves generated in two different principal incident wave directions. Good results appear to have been obtained in the multi-directional test for θ_p = 30°, T_p = 1.6 *s*, H_S = 15 *cm*. Figure 4.30 shows the directional spreading functions at the peak frequency f_p and 1.5 f_p. Definition of the directions with respect to the breakwater is shown in Figure 4.31. The incident wave field appears to have a principal direction of 35° rather than the 30° angle of incidence specified. This discrepancy may be the result of errors in the wave signal generation, or, more probably, the result of errors in directional measurement.

The principal reflected direction appears, from Figure 4.30, to be between 130° and 170°. A reflected direction of approximately 145° was expected, corresponding to the measured incident

direction of 35° and assuming the angle of reflection to be equal to the angle of incidence. This plot shows that the waves at frequency $f = f_p$ were reflected with a principal reflection angle of 50°, which is a more oblique angle than the angle of incidence. For the waves of frequency $f = 1.5\ f_p$ the principal angle of reflection was 10°, which is almost normal to the breakwater. These two angles differ considerably from but are centred around the expected reflection angle of 35°.

The amount of directional spreading in the reflected wave field is shown by Figure 4.30 to be higher than the spreading of the incident wave field. The reflected directional spectra show a lot of leakage of energy away from the principal direction, which may, or may not, indicate that the analysis program had difficulty in determining the shape of the spectra. Figure 4.32 shows the standard deviation of the incident and reflected directional spectra as a function of frequency. From this plot it is shown that the average σ_θ^2 of the incident spectrum is approximately 20° while for the reflected spectrum the average σ_θ^2 is approximately 45°. This indicates that the reflection of the incident wave field by the breakwater leads to a considerable amount of directional spreading.

The results of this test suggest that:

1) For intermediate and lower frequency waves, the principal angle of reflection is more oblique than the angle of incidence; while for higher frequency waves, which may or may not be present due to frequency scattering, the principal angle of reflection is less oblique than the angle of incidence.

2) Some directional spreading may be expected in the reflected wave field.

However, the analysis of the multi-directional test for $\theta_p = 15°$ did not provide meaningful results, possibly due to errors made in the operation of the experiment. Also, the analysis did not converge to give meaningful directional spectra for either of the uni-directional tests, however, the analysis program MLMWP was expected to give better results when applied to data with some spreading in direction rather than the uni-directional data used in these tests. This meant that the directionality

analysis was not able to be applied to measured signals from the regular uni-directional wave tests or the irregular uni-directional wave tests.

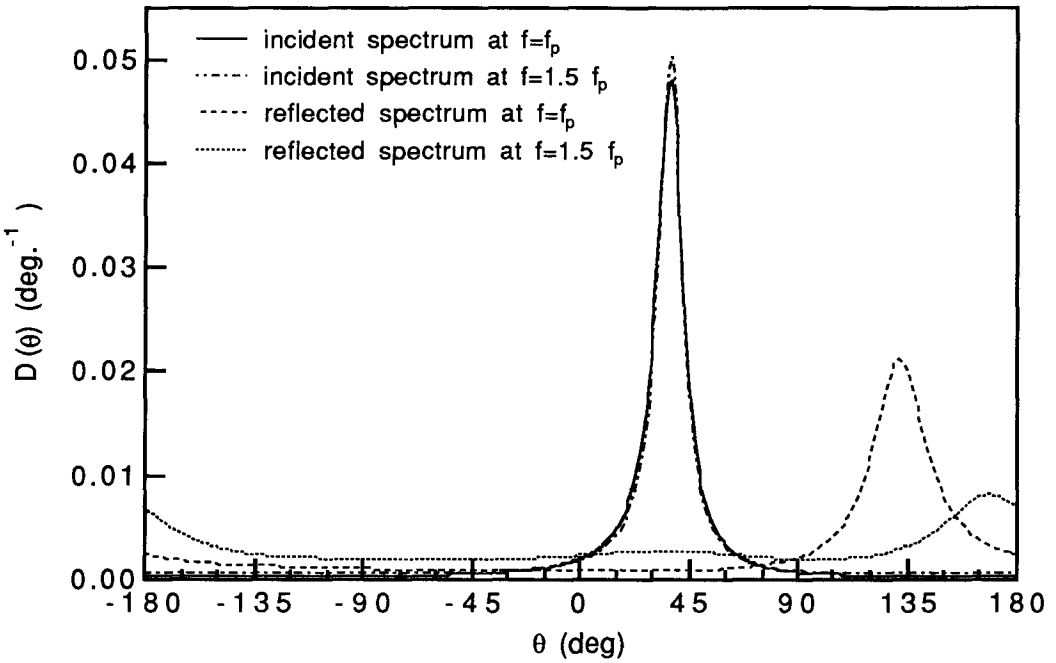

Figure 4.30 - Incident and reflected directional spreading functions for test 13, $\theta_p = 30°$

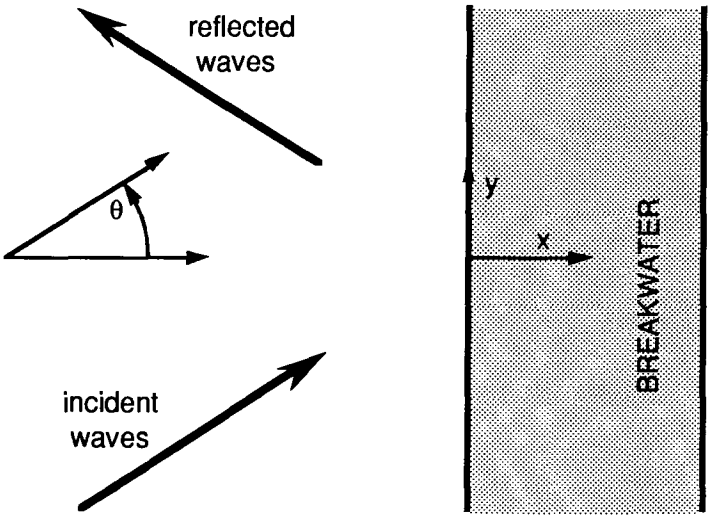

Figure 4.31- Definition sketch showing directions expressed as angles

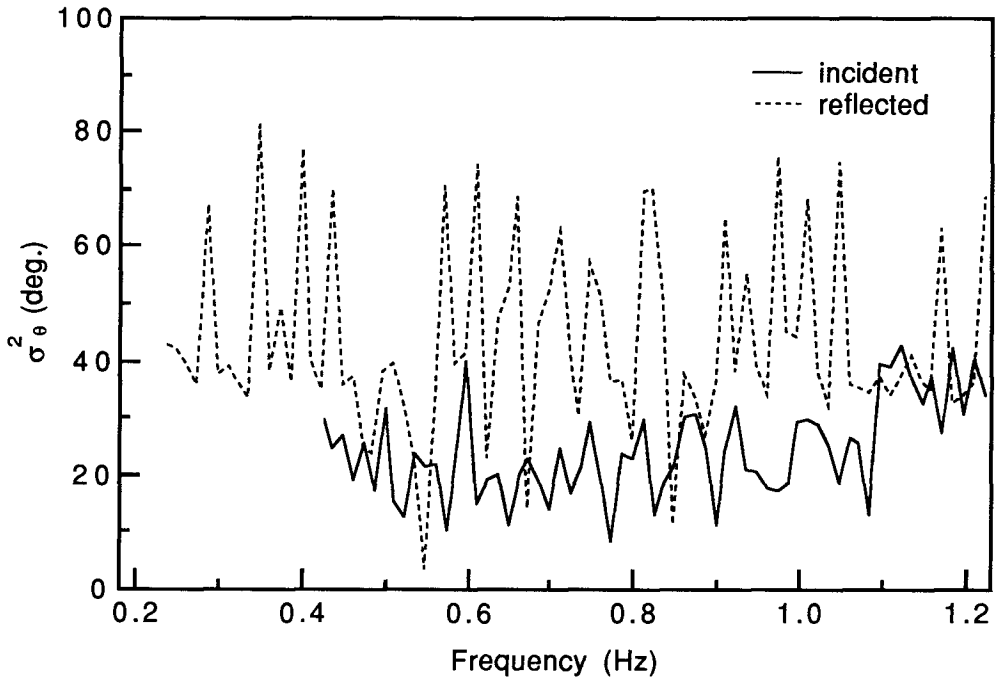

Figure 4.32 - Standard deviation of incident and reflected spreading functions for test 13, $\theta_p = 30°$

Chapter 5

CONCLUSIONS AND RECOMMENDATIONS

5.1 Reflection of Regular, Obliquely Incident Waves

Tests were undertaken using a range of regular, uni-directional waves obliquely incident on a model rubble-mound breakwater. A constant water depth of d = 0.5 *m* was used and waves were generated in four angles of incidence, $\theta = 0°, 30°, 45°$ and $60°$, with periods ranging from T = 1.0 *s* to 2.4 *s*, and heights of H = 5 *cm* to 19 *cm*. The selection of these wave characteristics resulted in a range in wave steepness parameter of H/L = 0.016 to 0.066, and depth to wavelength ratio of $d/gT^2 = 0.009$ to 0.051.

The model rubble-mound breakwater used was impervious, armoured with large size rocks, W > 1 *kg*, and front and back slopes of 1 : 1.5.

The reflection coefficient and the reflected phase lag, which describe the reflection characteristics of the breakwater, were estimated using a least squares method and measurements of water surface elevations from three probes. The least squares method, described by Mansard and Funke (1980) and Isaacson (1991), was extended in this study to analyse oblique wave reflection in a manner indicated by Isaacson (1991). This analysis method assumed that the wave field was described by linear wave theory and also assumed that there was no frequency or directional scattering in the reflection process and that the angle of reflection was equal to the angle of incidence. A frequency analysis and examination of the reflected wave records indicated that the assumption made about the frequency of the reflected wave field was valid. Insufficient evidence was found in the directionality analysis to prove or disprove the assumption that the angles of reflection and incidence were equal. Some evidence of directional scattering was found, however this is not thought to greatly affect the results from the regular wave analysis. The accuracy of the regular wave analysis method was examined and it was found to give good accuracy.

Results from the regular wave tests indicate that the reflection characteristics, K_r and β, are functions of the parameters depth to wavelength ratio d/gT^2 and angle of incidence θ. K_r and β were shown to be independent of wave height.

The measured reflection coefficients ranged from 10% to 59% for the range of incident waves generated. For each angle of incidence θ , K_r was presented as a function of d/gT^2. These results indicated that relationships which describe the reflection of normally incident waves do not adequately describe the reflection of obliquely incident waves. In general, K_r was shown to increase with increasing angle of incidence θ, especially for waves with higher values of depth to wavelength ratio d/gT^2. Results also indicated the presence of a minimum value of K_r related to a maximum proportion of wave energy dissipated by wave breaking on the breakwater. The lower proportion of energy dissipation observed in tests with more oblique angles of incidence was speculated to be the reason that K_r was observed to increase with θ.

Measured values of reflected phase lag β were in the range $\beta = 9°$ to $116°$. β was shown to be a function of d/gT^2, and increasing d/gT^2 was shown to lead to increased values of β. The shift in position of the standing wave pattern x' was observed to be approximately constant with changing values of d/gT^2 for all angles of incidence except for $\theta = 60°$. The study also indicated that β and x' increase with increasing angle of incidence θ.

5.2 Reflection of Irregular, Obliquely Incident Waves

Four irregular wave test were undertaken in this study with the objective of determining whether results obtained from regular wave tests would adequately describe irregular wave reflection. Waves were generated in two angles of incidence $\theta = 0°$ and $45°$ with constant water depth $d = 0.5$ *m,* constant peak frequency corresponding to $T_p = 1.6$ *s*, with spectral density approximately described by a Bretschneider spectrum, and $H_s = 6$ *cm* and 12 *cm.*

The water surface elevation signals measured without the breakwater in place were subtracted from the signals measured with the breakwater in place to get the reflected wave water elevation signals. Estimates of the incident and reflected spectral density were then obtained by analysing the incident and reflected wave elevation signals with a Fourier analysis program. Estimates of spectral density from three probes were smoothed using a moving average filter, then averaged. The reflection coefficient function $K_r(f)$ was estimated by dividing the reflected by the incident spectral density then taking the square root. The average reflection coefficient $\overline{K_r}$, was estimated for each test as the square root of the ratio of the zeroth moments of the reflected and incident spectral density.

The spectral density of the incident and reflected wave trains were compared and were seen to be close in shape, however the peaks of the reflected spectra were generally at a lower frequency than those of the incident spectra. Also, some incident wave energy appeared to be scattered to higher frequencies by the breakwater, resulting in higher amounts of reflected wave energy at frequencies of approximately twice the peak frequency than was expected from results of the regular wave tests.

The irregular reflection coefficient function $K_r(f)$ compared closely to the reflection coefficients measured for the regular wave tests. This comparison was not as close for waves of frequency $f > 0.6\ Hz$ and angle of incidence $\theta = 0°$. In general, the results from the regular wave tests closely described the reflection of the irregular waves.

Values of average reflection coefficient $\overline{K_r}$, ranging from 31% to 38% were measured. $\overline{K_r}$ was shown to be independent of significant wave height H_S, but dependent on angle of incidence θ. For angles of incidence $\theta = 0°$ and 45°, values of average reflection coefficient of $\overline{K_r} = 31\%$ and 38% were measured. These results indicate that in general K_r increases with increasing θ, reiterating the results of the regular wave tests.

5.3 Directionality of Incident and Reflected Wave Fields

The conclusions that were able to be taken from the directionality analysis were limited due to the inadequacy of the directional analysis method in analysing wave fields containing reflected wave energy. Reasonable results appear to have been obtained for test 13 with principal incident wave direction $\theta_p = 30°$. The results from this test indicate that the multi-directional incident wave field was reflected from the breakwater with an amount of directional spreading greater than that of the incident wave field. For this test, the principal angle of reflection was not equal to the principal angle of incidence for all frequencies, rather, results indicated that the angle of reflection was a function of frequency. Higher frequency waves were reflected at angles more normal than the angle of incidence, and lower frequency waves were reflected at angles more oblique than the angle of incidence.

5.4 Recommendations for Further Study

A review of the literature on wave reflection, undertaken during the initial stages of this study, revealed a lack of understanding of the reflection characteristics of oblique waves. This study has increased the level of understanding in this area. Relationships between the important parameters K_r, β, d/gT^2, and θ have been determined and discussed for the conditions chosen in this study, however there is a need for more experimental work to be done. In particular, experimental data is needed on oblique wave reflection from structures with different types of construction and face slopes over a range of incident wave angles.

More information is also needed on the directionality of reflected wave fields, including information on the amount of directional spreading in the incident and reflected wave fields and information on the principal direction of the reflected wave field. For this purpose, an improved method of directional wave analysis is needed which will estimate the incident and reflected directional spectra in wave fields containing significant amounts of reflected wave energy.

References

Allsop, N. W. H. and Hettiarachchi, S. S. L. (1988) "Reflections from Coastal Structures", Proc. 21st Coastal Engineering Conference, June, Costa del Sol-Malaga, Spain, pp.782-794.

Battjes, J. A. (1974) "Surf Similarity", Proc. 14th Coastal Engineering Conference, June, Copenhagen, Denmark, pp.466-480.

Delmonte, R. C. (1972) "Scale Effects of Wave Transmission through Permeable Structures", Proc. 13th Coastal Engineering Conference, July, Vancouver, Canada, pp.1867-1872.

Goda, Y. and Suzuki, Y. (1976) "Estimation of Incident and Reflected Waves in Random Wave Experiments", Proc. 15th Coastal Engineering Conference, July, Honolulu, Hawaii, pp.828-845.

Isaacson, M. I. (1991) "Measurement of Regular Wave Reflection", J. Waterway, Port, Coastal and Ocean Engineering, ASCE, vol.117, no.6, pp.553-569.

Jamieson, W. W. and Mansard, E. P. D. (1987) "An Efficient Upright Wave Absorber", Proc. ASCE Speciality Conference on Coastal Hydrodynamics, Newark, Deleware.

Kobayashi, N., Cox, D. T. and Wurjanto, A. (1990) "Irregular Wave Reflection and Run-up on Rough Impermeable Slopes", J. Waterway, Port, Coastal and Ocean Engineering, ASCE, vol.116, no.6, pp.708-726.

Mansard, E. P. D. and Funke, E. R. (1980) "The Measurement of Incident and Reflected Wave Spectra using a Least Squares Method", Proc. 17th Coastal Engineering Conference, March, Sydney, Australia, pp.154-172.

Mansard, E. P. D., Sand, S. E. and Funke, E. R. (1985) "Reflection Analysis of Non-Linear Regular Waves", Technical Report No. TR-HY-011, Hydraulics Laboratory, National Research Council of Canada, Ottawa, Canada.

Nwogu, O. (1989) "Analysis of Fixed and Floating Structures in Random Multi-Directional Waves", Ph.D. Dissertation, Department of Civil Engineering, University of British Columbia, Vancouver, Canada.

Seelig, W. N. and Ahrens, J. P. (1981) "Estimation of Wave Reflection and Energy Dissipation Coefficients for Beaches, Revetments, and Breakwaters", report no.TP 81-1, Coastal Engineering Research Centre, U. S. Army Engineer Waterways Experiment Station, Vicksburg, Mississippi.

Seelig, W. N. (1983) "Wave Reflection from Coastal Structures" Proc. Conference on Coastal Structures, ASCE, Arlington.

Shaver, M. D. (1989) "Regular Wave Conditions in a Directional Wave Basin", M.A.Sc. Thesis, Department of Civil Engineering, University of British Columbia, Vancouver, Canada.

Sollitt, C. K. and Cross, R. H. (1972) "Wave Transmission through Permeable Breakwaters", Proc. 13th Coastal Engineering Conference, July, Vancouver, Canada, pp.1827-1846.

Tautenhain, E., Kohlhase, S. and Partenscky, H. W. (1982) "Wave Run-up at Sea Dikes under Oblique Wave Approach", Proc. 18th Coastal Engineering Conference, November, Capetown, South Africa, pp.804-810.

Thornton, E. B. and Calhoun, R. J. (1972) "Spectral Resolution of Breakwater Reflected Waves", J. Waterway., Port, Coastal and Ocean Engineering, ASCE, vol.98, no.4, pp.443-460.

U. S. Army Corps of Engineers (1984) "Shore Protection Manual", Coastal Engineering Research Center, U.S. Army Engineer Waterways Experiment Station, Vicksburg, Mississippi.

Wilson, K. W. and Cross, R. H. (1972) "Scale Effects in Rubble-Mound Breakwaters", Proc. 13th Coastal Engineering Conference, July, Vancouver, Canada, pp.1873-1884.